Water Clusters
in Atmospheric Chemistry

Complexes and Clusters of Water Relevant to Atmospheric Chemistry: H₂O Complexes with Oxidants

Petr G. Sennikov,[b] Stanislav K. Ignatov,[c] and Otto Schrems*[a]

Experimental observations and data from quantum chemical calculations on complexes between water molecules and small, oxygen-containing inorganic species that play an important role as oxidants in the atmosphere ($O(^1D)$, $O(^3P)$, $O_2(X^3\Sigma_g)$, $O_2(b^1\Sigma_g{}^+)$, O_3, HO, HOO, HOOO, and H_2O_2) are reviewed, with emphasis on their structure, hydrogen bonding, interaction energies, thermodynamic parameters, and infrared spectra. In recent years, weakly bound complexes containing water have increasingly attracted scientific attention. Water in all its phases is a major player in the absorption of solar and terrestrial radiation. Thus, complexes between water and other atmospheric species may have a perceivable influence on the radiative balance and contribute to the greenhouse effect, even though their concentrations are low. In addition, they can play an important role in the chemistry of the Earth's atmosphere, particularly in the oxidation of trace gases. Apart from gas-phase complexes, the interactions of oxidants with ice surfaces have also received considerable advertency lately due to their importance in the chemistry of snow, ice clouds, and ice surfaces (e.g., ice shields in polar regions). In paleoclimate—respectively paleoenvironmental—studies, it is essential to understand the transfer processes from the atmosphere to the ice surface. Consequently, special attention is being paid here to the intercomparison of the properties of binary complexes and the complexes and clusters of more complicated compositions, including oxidants adsorbed on ice surfaces, where ice is considered a kind of large water cluster. Various facts concerning the chemistry of the Earth's atmosphere (concentration profiles and possible influence on radical reactions in the atmosphere) are discussed.

1. Introduction

Unique structural features of the water molecule—its small size, ability to form two-directional hydrogen bonds, and the presence of two lone electron pairs—determine the unique properties of liquid water and ice, as well as of many chemical processes involving water molecules in the gas phase and at the gas–liquid or gas–solid interfaces. As a rule, these processes are based on the formation of hydrogen-bonded water complexes with partner molecules of simple composition (1:1 or 1:2) or more complicated structures (1:n; $n > 2$), usually referred to as molecular clusters. In the last two decades, different aspects concerning the formation of these clusters, and their effect on various physical and chemical processes occurring in the atmosphere, have attracted considerable interest.[1–8] This is not surprising, because there is a considerable amount of water in the atmosphere, especially in the troposphere.

The concentration of water in the atmosphere is very dependent on altitude. It has been shown[9] that the partial pressure of water vapor usually decreases with altitude in the lowest atmospheric levels (troposphere), achieving a minimum in the tropopause, followed by a slight increase in the lowest part of the stratosphere. Such changes correspond to the well-known temperature inversion in the tropopause.[10] At the minimum (about 212 K) temperature in the tropopause, the water "freezes off" and its partial pressure corresponds to the saturated vapor pressure over the ice. Despite the fact that the temperature increases slightly in the lower stratosphere (about 15–20 km), only a small amount of water (5–6 ppm) reaches this altitude. However, an analysis of the prevalence data for some important molecular pollutants in the atmosphere, the energies (and, in some cases, thermodynamic functions) of formation of their complexes with H₂O molecules gives reasons for the assumption that these complexes can 1) be formed under such conditions and 2) play important roles in many complicated atmospheric processes. For example, water in all its phases is a major player in the absorption of solar and terrestrial radiation and is thus an important greenhouse gas.[6, 11, 12] Because water complexes are able to alter the radiative balance and chemistry of the atmosphere, the formation of complexes and clusters of water causes a shifting and broadening of monomer spectral features in absorption spectra, the appearance of new absorption bands, and an intensity enhancement of forbidden electronic transitions. These processes can lead, for example, to difficulties in the determina-

[a] Prof. Dr. O. Schrems⁺
Alfred Wegener Institute for Polar and Marine Research
Am Handelshaven 12, 27568 Bremerhaven (Germany)
Fax: (+49) 471-4831-1425
E-mail: oschrems@awi-bremerhaven.de

[b] Prof. Dr. P. G. Sennikov
Institute of Chemistry of High Purity Substances RAS
Tropinin str. 49, 603950 Nizhny Novgorod (Russia)

[c] Dr. S. K. Ignatov
Department of Chemistry, University of Nizhny Novgorod
Gagarin ave. 23, 603950 Nizhny Novgorod (Russia)

[⁺] Department of Chemistry, University of Bremen, Bremen (Germany)

Prof. Dr. Sc. Petr Sennikov was born in 1951 in Nizhny Novgorod (formerly Gorky, Russia). He obtained his diploma in chemistry (1973) from the N.I. Lobachevsky State University of Nizhny Novgorod. After obtaining his Ph.D. in physical chemistry (1980) at the same University, he became Assistant Professor of Chemistry at The Pedagogical Institute of Nizhny Novgorod. Since 1985, he has been the Head of the Laboratory of Molecular Spectroscopy at the Institute of High-Purity Substances at the Russian Academy of Sciences. His research interests include experimental (UV, IR, and MW spectroscopy) and theoretical studies of weakly bound systems; application of high-resolution IR and MW spectroscopy to the analysis of volatile compounds, and gas-phase reaction mechanisms of inorganic species.

Dr. Stanislav Ignatov was born in 1965 in Nizhny Novgorod, Russia. He obtained his diploma in chemistry (1989) from the N.I. Lobachevsky State University of Nizhny Novgorod. After his Ph.D. in physical chemistry (1995), obtained at N.N. Semenov Institute of Chemical Physics (Moscow), and a postdoctoral fellowship with Professor Alexander Bagatur'yants (Center of Photochemistry of RAS, Moscow), he was appointed Assistant Professor of Spectroscopy at the University of Nizhny Novgorod. His research interests include quantum chemistry of weakly bound complexes and adsorption systems, thermodynamics, and kinetics and reaction mechanisms of gas-phase and surface reactions of inorganic species.

Prof. Dr. Otto Schrems obtained diplomas in chemical engineering and chemistry and received his Ph.D. in Physical Chemistry in 1981 from the University of Marburg (Germany). He worked as Honorary Research Fellow at the University College London with Professors D. J. Millen and A. C. Legon, as a scholarship holder at the University of California in Berkeley with Prof. G. C. Pimentel, and at the Université Pierre et Marie Curie in Paris with Prof. J. P. Perchard. In 1987, after working for three years as a senior scientist at the University of Siegen (Germany) with Prof. E. Knözinger, he was appointed Professor of Atmospheric Chemistry at the University of Bremen and as head of the Atmospheric Chemistry Division at the Alfred Wegener Institute of Polar and Marine Research in Bremerhaven. His main research interests include polar and marine atmospheric chemistry, intermolecular forces, molecular complexes, molecular spectroscopy and remote sensing.

tion of pollutants in the atmosphere by remote laser techniques. To a great extent, clusters of water involved in photochemical processes can also modify monomer dissociation pathways and lead to entirely new photodissociation channels. Some aspects of the role of small water clusters (mainly 1:1 complexes) in atmospheric processes have been reviewed recently.[2,8] The role of water dimers in the atmosphere is an important—but still controversial—issue that has yet to be resolved.

It should also be emphasized that complexes played an important role in the early Earth's atmosphere. The kinetic parameters influenced by complex formation (frequently under higher concentrations of many reactants than is present nowadays) could change the reaction channels so crucially that the atmospheric reactions could result in quite different compositions of the atmosphere, depending on the reactivity of complexes. Thus, the kinetic and thermodynamic properties of atmospheric complexes should be taken into account during the development of time-evolution models of the Earth's atmosphere.

The complicated physicochemical processes—with the participation of trace gases—that occur both on the surface of small ice particles in the troposphere (cirrus clouds) and in the stratosphere (polar stratospheric clouds, PSCs) as well as on snow surfaces and the surface of glacier ice shields at the Earth's poles are also of great interest. Some recent reviews[13–15] are mainly dedicated to the physical aspects of these processes.

Herein, we review the literature on the experimental and theoretical studies on molecular complex formation between water molecules and atmospheric trace gases of a very important class—those containing oxygen atoms. Among these, we will focus on the main components of the atmosphere—molecular oxygen, ozone (whose role in atmospheric processes is extremely important), and the products of oxygen and ozone photolysis that occur in the atmosphere, including the photolytic reactions occurring with the participation of the water molecule. Thus, in summary, we review the investigations which have studied the complexes of water with $O(^1D)$, $O(^3P)$, $O_2(X^3\Sigma_g)$, $O_2(b^1\Sigma_g^+)$, O_3, HO, HOO, HOOO, and H_2O_2.

The most interesting results are related to the interaction of the above-mentioned species with water clusters and, at the limit, with liquid or solid water surfaces. Unfortunately, a literature analysis shows that such data is still very rare. Thus, it seems reasonable to supplement this review with literature data concerning ice clusters or ice surfaces with adsorbed trace gas molecules. From a structural point of view, the ice surface models used in many theoretical works are just examples of water clusters constructed in agreement with special rules ("ice rules") which can of course be realized in the atmosphere. Concerning the investigations involving ice surfaces, we refer to those studying the structure and energies of adsorption complexes, which are model species of real water clusters that could exist in the atmosphere and, thus, are connected directly to the main goal of this overview.

Over the past decades, many studies devoted to the chemistry of ions and their complexes in the gas phase have been

performed. However, because the experimental approaches for studying ionic processes in the gas phase are quite different from the conditions suitable for atmospheric studies, we consider here only the neutral structures, with emphasis on infrared and microwave spectroscopy, matrix isolation, and quantum chemical methods.

This review is divided into sections dedicated to complexes of oxygen (both molecular and atomic), ozone, hydrogen-containing radicals (HO, HOO, HOOO), and hydrogen peroxide. Throughout, we designate the binding energy as ΔE, determining it as the difference between the sum of the energies of nondistorted, noninteracting monomers and the energy of the complex. In the case of *n*-molecular clusters, "the monomers" means a trace molecule and a free, nondistorted cluster of $n-1$ remaining water molecules. In many theoretical studies (unfortunately, however, not in all), the binding energies are supplemented with ΔE values corrected by the basis set superposition error (BSSE). The BSSE-corrected values take into account the basis set incompleteness (which artificially increases the binding energy) and will be designated (if any) as ΔE_{CP}.

2. Theoretical and Experimental Studies of Oxidant–Water Complexes

2.1. Complexes of H$_2$O with Molecular Oxygen

The possibility of weak complex formation between dioxygen (O$_2$) and H$_2$O molecules was indicated for the first time in early theoretical studies in the middle of the 1980s.[16–19] In these studies, it was proposed that this kind of complex is of van der Waals type with C_{2v} symmetry. Different structures of C_{2v} symmetry were examined theoretically [20,21] using levels of theory up to MP2(full)/6-311++G(2d,p) and CASSCF(10,7)/6-311++ G(2d,p).[21] On the basis of these results, the role of the oxygen complexes with water was discussed primarily in order to explain the experimentally observed spectral features of water vapor in the UV wavelength range. Later, however,[22,23] an analysis of vibrational frequencies showed the presence of imaginary values in the above complexes, indicating that C_{2v} structures do not correspond to the true minimum. Svishchev and Boyd[23] added the hydrogen-bonded configuration of C_s symmetry to the structure considered earlier and found, in the MP2(full)/6-311++G(2d,2p) optimization, that the most favorable conformation of this complex has a low-symmetry (C_s) hydrogen-bonded bent structure (Figure 1). This structure corresponds to the true minimum with a binding energy of about 2.9 kJ mol^{-1} (BSSE-corrected value: 2.1 kJ mol^{-1}). Energy improvements were also performed using the MP4(full) and B3LYP theories at the MP2(full)/6-311++G(2d,2p) optimized structures. The binding energy obtained at the highest level of theory MP4(full)/6-311++G(2d,2p)//MP2(full)/6-31++G(2d,2p) is $\Delta E = 3.1$ kJ mol^{-1} and $\Delta E_{CP} = 2.7$ kJ mol^{-1}.

The conclusion on the hydrogen-bonded nature of the H$_2$O·O$_2$ complex was confirmed recently with a QCISD/6-311++G(2d,2p) optimization.[24,25] The optimized structure (see Figure 1), which is close to those found by Svishchev and Boyd,[23] has C_s symmetry and a binding energy of 2.9 kJ mol^{-1}. Unfortunately, the BSSE-corrected value was not reported. On the basis of additional CASSCF and MRCI calculations, the vertical excitation energies of the low-lying singlet states of this complex were also studied in this work. It is interesting that the MP2 and QCISD calculations gave rather different values of O—H···O and H···O—O angles: at the MP2 level, the O—O bond is nearly parallel to the O—H··· line, whereas at the QCISD level, the O—O bond is close to the direction of the bisector line of the H—O—H of water, probably as a result of the dipole polarizability energy term.

Quite recently, Sabu et al.[26] performed a quantum chemical study of a detailed potential energy surface (PES) of the H$_2$O·O$_2$ complex at the MP2 MRSDCI levels with aug-cc-pVTZ basis. In agreement with previous studies, they concluded that the most stable structure is the one with C_s symmetry, close to the QCISD/6-311++G(2d,2p) geometry of Kjaergaard et al.[25] The uncorrected binding energy of the global minimum was estimated to be 2.01 kJ mol^{-1}. On the basis of analyzing the PES, they concluded that the near-linear, H-bonded conformation (HO—H···O—O) is 0.54 kJ mol^{-1} higher in energy and, in contrast with previous MP2 results, the C_{2v} cyclic configurations with two H-bonds are not true minima of this complex. This conclusion is in good agreement with the results of Fourier-transform microwave spectroscopy.[27]

The infrared (IR) spectrum of the complex has been calculated,[23] and the thermodynamic functions of the complex formation under standard conditions (298.15 K and 101.325 kPa) estimated: $\Delta H_f = 1.33$ kJ mol^{-1}; $\Delta S_f = -0.046$ J K^{-1} mol^{-1}; $\Delta G_f = 15.12$ kJ mol^{-1}. Using these data, the equilibrium concentration of the H$_2$O·O$_2$ complex in the atmosphere (under standard conditions) was estimated to be 4.8 ppm. The authors pointed out that this value is higher than concentrations of many important atmospheric components, such as CH$_4$ (1.7 ppm), N$_2$O (0.31 ppm), CO (0.03–0.02 ppm), and fluorine-containing hydrocarbons (0.01–0.6 ppb), which play a key role in the greenhouse effect. On the basis of the available literature data on the thermodynamic functions of the H$_2$O·O$_2$ heterodimer and the prevalence of individual components, a concentration–altitude profile of the dioxygen–water complex has been calculated by these authors. Because the mole fraction of molecular oxygen is practically constant with altitude, the concentration profile of H$_2$O·O$_2$ is controlled by the abundance of water vapor (see Figure 2). This is clearly evident near the Earth's surface, where the concentration of H$_2$O·O$_2$ is practically equal to
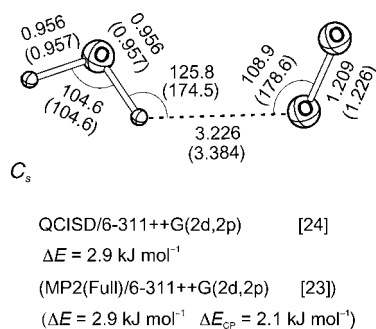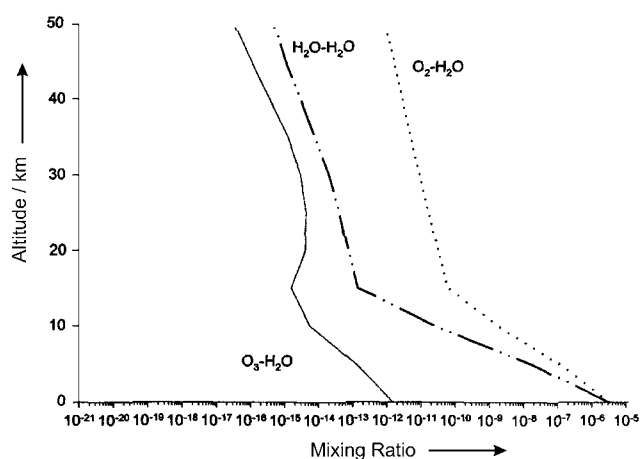

0.956
(0.957)

(0.956)
(0.957)

125.8
(174.5)

108.9
(178.6)

104.6
(104.6)

1.209
(1.226)

3.226
(3.384)

C_s

QCISD/6-311++G(2d,2p)   [24]

$\Delta E = 2.9$ kJ mol^{-1}

(MP2(Full))/6-311++G(2d,2p)   [23])

($\Delta E = 2.9$ kJ mol^{-1} $\Delta E_{CP} = 2.1$ kJ mol^{-1})

Figure 1. *Structure of the H$_2$O·O$_2$ complex*

Figure 2. Estimated mixing ratios of $H_2O \cdot O_2$, $H_2O \cdot O_3$, and $H_2O \cdot H_2O$ (for comparison) complexes as a function of altitude (Reproduced with permission from ref. [2]).
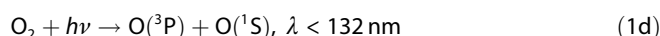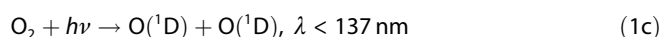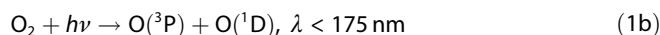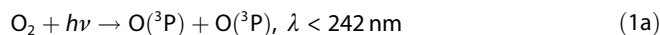
the concentration of the water dimer. The molar fractions of $H_2O \cdot O_2$ and $H_2O \cdot H_2O$ in the troposphere decrease quickly with altitude: The decrease is more significant for the water dimer because of the sharp decrease in the concentration of both components of the dimer. In the tropopause region, the molar fractions of H_2O and O_2 are practically constant and the concentration profiles of $H_2O \cdot O_2$ and $H_2O \cdot H_2O$ are similar to each other. Because the partial pressure of oxygen in the atmosphere is much higher than that of water, the molar fraction of the water dimer is several orders of magnitude less in comparison with the molar fraction of the $H_2O \cdot O_2$ complex, despite its low binding energy.

It is obvious, however, that the absolute concentration values should be considered with caution, because the approximations used in the thermodynamic calculations—first of all, the RRHO (rigid rotor–harmonic oscillator) approximation—are too crude to give accurate thermodynamic values for the weakly-bonded complexes, as has recently been shown, for example, for the H_2O dimer.[28] Accurate calculations of the mole fractions should obligatorily take into account (at least in an approximate manner) the effects of anharmonicity, internal rotations, and large-amplitude motions of coordinated molecules, which have a significant influence on the equilibrium constants. The above-mentioned studies do not take into account these corrections and, thus, the obtained results probably underestimate the concentrations of the complex.
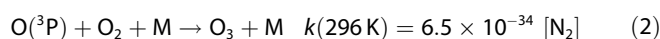
Because the absorption of the $H_2O \cdot O_2$ complex has a large effect on the water vapor continuum in the near-infrared region of the Earth's atmosphere, there was a recent attempt to model the form and optical depths of the continuum on the basis of known (mostly quantum chemical) estimates of absolute IR intensities and frequencies of water complexes with oxygen, nitrogen, and argon.[29] However, these authors concluded that "the comparisons are largely qualitative rather than quantitative due to the large uncertainty in the complexes' equilibrium constants…". Thus, there is obvious motivation to continue studying the $H_2O \cdot O_2$ and other water com-

plexes, in order to obtain more reliable estimates for both thermodynamic properties and spectral parameters.

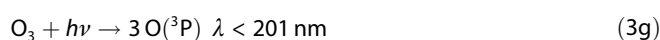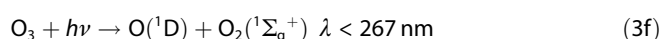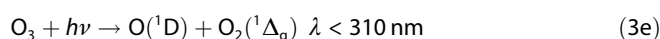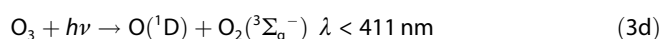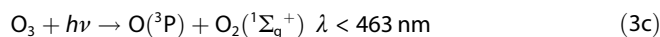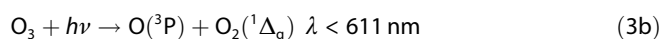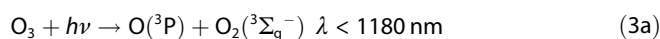Under the solar irradiation in the middle atmosphere, the oxygen molecules are transferred into excited states and participate in various photochemical reactions. Among the photolytic reactions, four basic channels of photodissociation resulting in atomic oxygen formation prevail [Eqs. (1a)–(1d)][30]

$$O_2 + h\nu \rightarrow O(^3P) + O(^3P), \quad \lambda < 242\ nm \tag{1a}$$

$$O_2 + h\nu \rightarrow O(^3P) + O(^1D), \quad \lambda < 175\ nm \tag{1b}$$

$$O_2 + h\nu \rightarrow O(^1D) + O(^1D), \quad \lambda < 137\ nm \tag{1c}$$

$$O_2 + h\nu \rightarrow O(^3P) + O(^1S), \quad \lambda < 132\ nm \tag{1d}$$

The triplet oxygen atoms initiate further reactions with oxygen molecules, resulting in the formation of ozone [Eq. (2)][31]

$$O(^3P) + O_2 + M \rightarrow O_3 + M \quad k(296\ K) = 6.5 \times 10^{-34}\ [N_2] \tag{2}$$

In turn, the ozone photolysis in the gas phase can lead (with different quantum yields and wavelength thresholds) to the formation of oxygen atoms and molecules in different spin and electronic states [Eqs. (3a)–(3g)][32]

$$O_3 + h\nu \rightarrow O(^3P) + O_2(^3\Sigma_g^-)\ \lambda < 1180\ nm \tag{3a}$$

$$O_3 + h\nu \rightarrow O(^3P) + O_2(^1\Delta_g)\ \lambda < 611\ nm \tag{3b}$$

$$O_3 + h\nu \rightarrow O(^3P) + O_2(^1\Sigma_g^+)\ \lambda < 463\ nm \tag{3c}$$

$$O_3 + h\nu \rightarrow O(^1D) + O_2(^3\Sigma_g^-)\ \lambda < 411\ nm \tag{3d}$$

$$O_3 + h\nu \rightarrow O(^1D) + O_2(^1\Delta_g)\ \lambda < 310\ nm \tag{3e}$$

$$O_3 + h\nu \rightarrow O(^1D) + O_2(^1\Sigma_g^+)\ \lambda < 267\ nm \tag{3f}$$

$$O_3 + h\nu \rightarrow 3\ O(^3P)\ \lambda < 201\ nm \tag{3g}$$

The oxygen atoms formed can interact with water molecules and initiate radical processes (discussed in the next section), or form molecular complexes.

There are no experimental observations or theoretical studies on the binary complexes of water with dioxygen in the excited state, except the studies dedicated to the UV spectra of O_2 coordinated with water.[19,21,22]. However, in these studies, the structure of the excited complex is not the subject of investigation and, as a rule, corresponds to the structure of the ground state.

A density functional theory (DFT) consideration of the interaction between molecular oxygen, both in the triplet ($^3\Sigma_g^-$) and singlet ($^1\Sigma_g^+$, erroneously referred to as $^1\Delta_g$ in ref. [33]) spin states, and water clusters (icelike in structure) has recently

been given.[33] The clusters contained up to nine water molecules of the ice, *Ih* in structure, with the boundary atoms fixed in the crystalline positions. A full geometry optimization was performed for the central part of the clusters including the interacting oxygen molecules. The singlet and triplet oxygen molecules placed at the surface and inside the cages of the cluster tended to move outside. No complex structures with pronounced hydrogen bonds were found for the singlet and triplet states of the oxygen molecule. It was concluded that the dioxygen molecules are only physically adsorbed at the surface of the ice crystal. This conclusion is in agreement with the small binding energy of the binary complex (2–3 kJ mol^{-1}) found in the above-described studies.[23–25]

2.2. Complexes of H$_2$O with Atomic Oxygen

Atomic oxygen in the ground (^{3}P) electronic state formed during the ozone photolysis in Equation (1) can interact with water vapor by forming weakly bound complexes between O-(^{3}P) and a water molecule. This process has been investigated in detail in matrix isolation studies and quantum chemical calculations.[34,35] It was found that the HO• radicals formed from the photolysis of H$_2$O$_2$ (under 193 nm laser irradiation) in an argon matrix form a hydrogen-bonded complex between a water molecule and a triplet oxygen atom H–O–H···O(^{3}P) in high (80%) yield.[34] This complex has been studied by IR spectroscopy combined with quantum chemical calculations at the MP2 level in various basis sets up to 6-311++G(3d,3p).[35] The quantum chemical calculations performed at the UMP2/6-311++G(3d,3p) level confirmed the structure and the assignment of IR absorption bands proposed on the basis of the experimental study. The optimized geometry of the complex
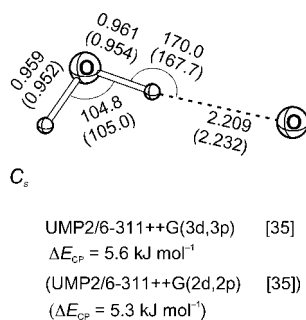

UMP2/6-311++G(3d,3p)   [35]
$\Delta E_{CP} = 5.6$ kJ mol^{-1}
(UMP2/6-311++G(2d,2p)   [35])
($\Delta E_{CP} = 5.3$ kJ mol^{-1})

Figure 3. *Structure of the H$_2$O·O(^{3}P) complex.*

corresponds to the open hydrogen-bonded bent structure shown in Figure 3. The optimized hydrogen bond length at the best level of theory is 2.209 Å. It was established experimentally that the IR absorption bands of the stretching vibrations of the coordinated water molecule are red-shifted by only 4–5 cm^{-1}, which can be considered as evidence of the formation of a weak intermolecular bond. In agreement with this result, the best theoretical estimate of the BSSE-corrected binding energy is 5.60 kJ mol^{-1}. The frequency calculations were also performed for all the deuterated analogs. The calcu-

lated frequency shifts (typically 5–26 cm^{-1}) were also in good agreement with the observed ones (5–22 cm^{-1}).

In contrast with O(^{3}P), the existence of a stable complex between O(^{1}D) and H$_2$O is still an open and intriguing question. The reason for this is a long-lasting discussion about the existence of (and possibility of observing) a special kind of singlet molecular complex H$_2$O·O, with the O···O-coordinated structure known as water oxide or oxywater. This structure was proposed for the first time in early studies on the structure of H$_2$O$_2$, in an attempt to explain the high dipole moment of H$_2$O$_2$ observed in the experiment.[36] This proposal, however, was refuted when the skew structure of H$_2$O$_2$ was established. In 1955, Bain and Giguerre[37] proposed the existence of new tautomeric forms of H$_2$O$_2$ and undertook a special investigation in order to detect them on the basis of IR spectra of H$_2$O$_2$ isotopomers, but failed. Later, the concept of the participation of oxywater as an intermediate of oxidative processes was frequently used in many studies.[36] However, to date, oxywater has never been observed experimentally. In 1966, Kalder and Shavitt[38] performed a self-consistent field (SCF) molecular orbital (MO) study of this structure in a minimal basis set and found that the formation of oxywater from H$_2$O$_2$ is quite unfavorable from an energetic point of view. In 1983, Pople's group optimized this structure[39] and found that oxywater has a stable minimum at the HF/6-31G(d) level. However, the activation barrier of the rearrangement from H$_2$OO to H$_2$O$_2$ was negligibly small when correlation effects were taken into account. The energy of oxywater was estimated at the correlated level to be about 220 kJ mol^{-1}, relative to H$_2$O$_2$.[40] It was shown, for the first time, in studies[41,42] concerning the reaction mechanism of ammonia oxidation, that oxywater is a true minimum on the PES with a barrier of rearrangement of about 20 kJ mol^{-1}. The most reliable confirmation of this fact came from studies by Schaefer and co-workers[43,44] who performed the full geometry optimization of oxywater, hydrogen peroxide, and the transition structure between them at the MP2, MP4, CCSD, CCSD(T), and BD levels in the DZP and TZ2P basis sets. (Hereafter, the DZ, DZP, TZP, and TZ2P+f designate the "double-zeta", "double-zeta + polarization function", "triple-zeta + polarization function", and "triple-zeta + two d,p-functions + f-function" basis sets. Thus, they correspond (exactly or approximately) to the 6-31G, 6-31G(d,p), 6-311G(d,p), and 6-311G(2df,2p) basis sets in the widely-used notation of Pople). The best estimate of the energy of oxywater (obtained at the CCSD(T)/TZ2P+f level)[43] is 195.8 kJ mol^{-1}, relative to H$_2$O$_2$. The activation barrier was estimated to be 23.8 kJ mol^{-1}, the ZPE correction reduces it to 13.8 kJ mol^{-1}. The optimized structure is shown in Figure 4. Later, the oxywater structure and energy
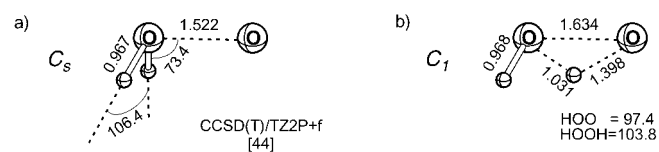
a)

CCSD(T)/TZ2P+f
[44]

b)

HOO = 97.4
HOOH = 103.8

Figure 4. *a) Structure of the H$_2$O·O(^{1}D) complex and b) the transition state in its rearrangement to H$_2$O$_2$.*

were also studied using DFT and G2 theory[45] and the results are in good agreement with refs. [43,44].

Thus, the final conclusion of the studies reported to date is that oxywater in the gas phase is an unstable species characterized by an extremely flat and shallow minimum at the potential energy hypersurface corresponding to the C_s structure. Comparing the energy of $O(^1D)$ formation with the corresponding value of H_2O_2, the binding energy of that $H_2O \cdot O(^1D)$ complex is estimated to be 155.2 kJ mol^{-1}, whereas the activation energy of rearrangement to H_2O_2 is only 23.8 kJ mol^{-1}. The large amount of energy resulting from complex formation combined with a negligible reaction barrier for rearrangement explains why no evidence has been found for oxywater in the atmosphere.

Okajima[46] made an attempt to explain the possible participation of oxywater in the soft oxidation of bioorganic molecules, using an idea about the proton-relay mechanism of oxywater formation when source H_2O_2 is surrounded by several water molecules. In this case, the heat of oxywater formation from H_2O_2 can be dramatically decreased due to solvation effects when additional water molecules are coordinated with oxywater. For example, ΔH_0 calculated at the B3LYP/6-311++G(d,p) level decreased from 190.8 kJ mol^{-1} for free oxywater to 113.4 kJ mol^{-1} for oxywater with three coordinated water molecules. However, the activation energy of rearrangement also decreased (from 30.5 to 10.0 kJ mol^{-1}), making oxywater less stable from a kinetic point of view. Similar results were obtained at the MP2 level for a 1:2 oxywater–water cluster.

The interaction of $O(^1D)$ with icelike water clusters has also been studied by Ignatov et al.[33] using a model cluster of eight water molecules. A geometry optimization shows that $O(^1D)$ does not break the O—H bonds as is expected for the gas-phase. Instead, the energetically very profitable complex with one of the internal H_2O molecules (unfixed in this model) with an O···O distance of about 1.5 Å and a valence angle HOH of

boring water molecules. The four additional hydrogen bonds formed with the neighboring water molecules of the cluster decrease the energy of the oxywater structure to 110.9 kJ mol^{-1} (relative to H_2O_2 inside the cluster) whereas the gas-phase energy (relative to a free H_2O_2 molecule) is 191.6 kJ mol^{-1} (G2 calculation) and 189.1 kJ mol^{-1} (B3LYP/6-31+G(2d,2p)). It should be noted that the activation barrier for the rearrangement to H_2O_2 is 70.2 kJ mol^{-1}. This is a much higher value than the corresponding values in the gas phase or in cyclic clusters as considered by Okajima.[46] The explanation for the large difference between the two structures is the existence of additional hydrogen bonds inside the icelike cluster. As is evident from the calculations,[33] the stabilization of oxywater may take place in a solid medium which can form multiple hydrogen bonds with the oxygen atom. The authors proposed that attempts to observe oxywater or related complexes should probably be concentrated on solid state observations of oxygen-containing molecules having bulky substituents and the ability to form hydrogen bonds with the substrate. It is interesting that the calculated spectra of the oxywater structures embedded into the water network give extremely low frequencies located in the region close to the position of the band at 2860 cm^{-1} observed experimentally ($\nu_2 + \nu_6$ combination band of H_2O_2).
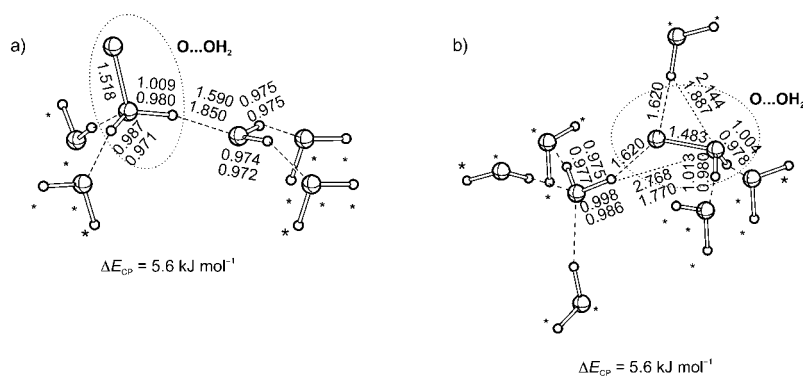
2.3. Complexes of H_2O with Ozone

Although the reactivity of ozone is of great interest in many fields of chemistry, there are only a few studies dedicated to the study of its complexes with small molecules including water.

The results of structure investigations for the $H_2O \cdot O_3$ complex obtained by the methods of gas-phase microwave spectroscopy[47] and low-temperature matrix isolation spec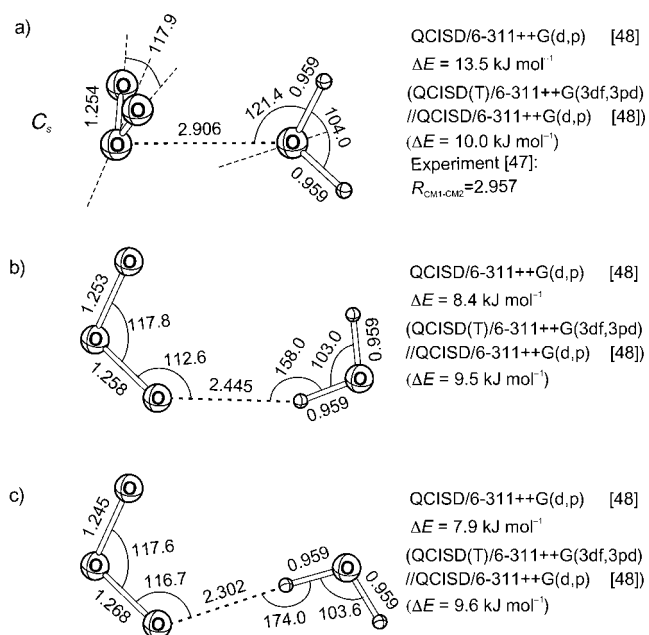troscopy[48,49] were published almost simultaneously. It was found[47] that the structure of this complex in the gas phase (in a pulsed ultrasonic jet) has C_s symmetry (close to the structure shown in Figure 6a): The water molecule and the central oxygen atom of the ozone molecule are located in the symmetry plane of the complex, with the hydrogen atom of water directed to the terminal oxygen atom of ozone. Such a structure is characterized by the opposite directions of the dipole moments of two monomers leading to the conclusion that the dipole–dipole electrostatic interaction gives the main contribution to the binding energy. This result was confirmed by quantum chemical calculations at the MP2/6-31G(d,p) level. The C_s symmetry of this structure is defined by the Coulomb interaction between the positively charged

Figure 5. Structure of a complex of $O(^1D)$ with an ice cluster: a) surface structure; b) structure inside the cluster. The lower values are the bond lengths of an undistorted cluster. Asterisks mark the atoms fixed in the optimization. Optimization at the B3LYP/6-31++G(d,p) level, energy calculation at B3LYP/6-311++G(2d,2p)/B3LYP/6-31++G(d,p).

about 116° was formed. The geometry of the optimized complex (shown in Figure 5) corresponds to the oxywater structure O···OH$_2$ forming four additional hydrogen bonds with neigh-

Figure 6. Possible conformations of the $H_2O \cdot O_3$ complex: a) dipole–dipole interacting structure; b) cis-structure; c) trans-structure.

hydrogen atom and two negatively charged oxygen atoms of the ozone molecule. The binding energy estimated at the MP2/6-31G(d) level is 14.9 kJ mol^{-1} ($\Delta E_{CP} = 2.9$ kJ mol^{-1}), the MP4/6-31G(d) constrained optimization (with monomer geometry taken from MP2/6-31G(d) calculation) gives $\Delta E = 10.0$ kJ mol^{-1}, $\Delta E_{CP} = 4.2$ kJ mol^{-1}.

Another structure (open OO–O···H–OH conformation with a long O–O distance) of the complex was found for the first time by Zacharov et al.[50] on the basis of an MP4/4–31G(d,p) optimization. Although the level of theory was obviously not appropriate to make a solid conclusion about subtle energetic differences, the authors draw attention to the important fact that the most abundant structure in the atmosphere is not the one with the lowest energy, but is the structure having the lowest Gibbs free energy at a given temperature. If the energy difference between the conformations is small, the most thermodynamically favorable form is probably the one with the longest O–O distance.

Recently, a geometry optimization of the 1:1 ozone–water complex has been carried out at the QCISD/6-311++G(d,p) level.[51] The calculations indicate that three structures (Figures 6a–c) are the stable forms of the $H_2O \cdot O_3$ complex. The most favorable structure (Figure 6a) of $H_2O \cdot O_3$ has C_s symmetry where the central oxygen atom of O_3 and all the atoms of H_2O are located on the molecular C_s plane (close to the structure found by Gillies et al.[47]). The dipole of H_2O is oriented towards the central oxygen atom of O_3. The other two conformations are *cis* and *trans* forms of $H_2O \cdot O_3$ (similar to the forms considered by Zacharov et al.[50]) where all the atoms are located on the molecular plane, and a hydrogen of H_2O binds to one of the terminal oxygen atoms of O_3 by a hydrogen bond. The binding energies of O_3 to H_2O for the dipole, *cis*, and *trans*

forms were calculated to be 13.5, 8.4, and 7.9 kJ mol^{-1}, respectively, at the QCISD/6-311++G(d,p) level, and 10.0, 9.5, 9.6 kJ mol^{-1} at the QCISD(T)/6-311++G(3df,3pd)//QCISD/6-311++G((d,p) level. Thus, the dipole-orientated form is more favorable in energy than the *cis* and *trans* conformations. However, the relative stability of the *cis* and *trans* complexes is still not well-established. Unfortunately, the authors did not report the BSSE-corrected values, which can be significantly lower. Rotational constants for the dipole-oriented form were calculated to be $A = 11.897$, $B = 4.177$, and $C = 3.318$ Ghz, which are in good agreement with the experimental values ($A = 11.961$, $B = 4.174$, and $C = 3.265$ GHz). On the other hand, the rotational constants for the *cis* and *trans* forms were only in poor agreement. These results indicate strongly that the dipole form of the complex is a strong candidate for the structure of $H_2O \cdot O_3$ observed experimentally in the gas phase.[51]

In an argon matrix, the binary ozone–water complex is characterized by a 3.3 cm^{-1} blue-shift of the ν_3 band of the ozone molecule and by a red-shift of the ν_3 band of water. The authors[48] concluded that the binding arises between the oxygen atom of the water molecule and the central oxygen atom of ozone. On the other hand, force-field calculations point to the inequality of two OH oscillators of water. It can appear in the case of the formation of a weak hydrogen bond in H–O–H···O$_3$. In these studies, ozone–water complexes of more complicated composition than the binary ones were also identified. Thus, for the complex $H_2O \cdot (O_3)_2$, the absorption band of the antisymmetric stretching vibration ν_3 of the water molecule was shifted by 30 cm^{-1}, and a new band at 3620 cm^{-1} appeared.
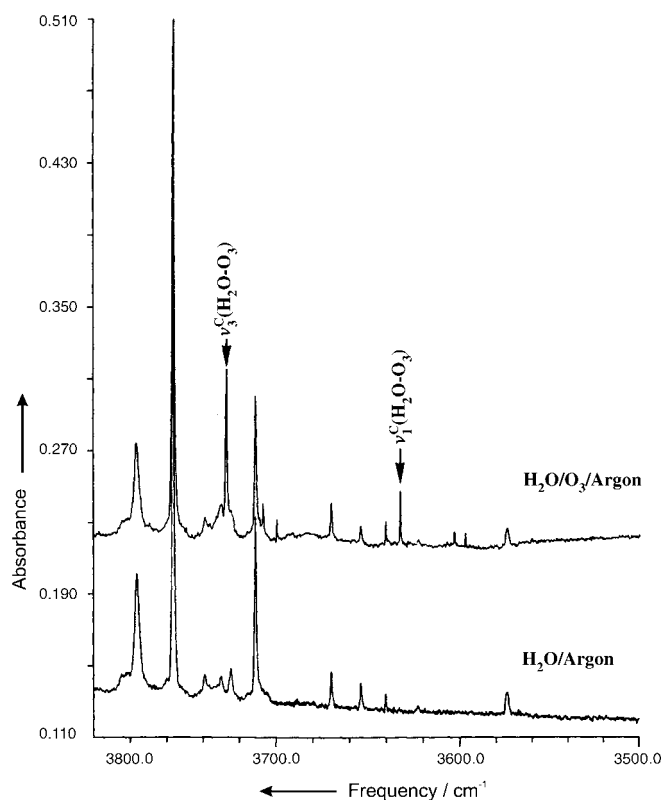
The 1:1 complex between water (H_2O, D_2O, HDO, $H_2^{18}O$) and ozone (O_3, $^{18}O_3$, $^{16,18}O_3$) in argon matrices and narrow band photolysis ($\lambda = 250$ nm) of this reaction system have been studied by Jaeger[52] by means of Fourier transform infrared (FTIR)

Table 1. Observed IR absorption bands of the ozone–water complex [cm^{-1}] in an argon matrix.[49, 52] (The corresponding IR shifts relative to monomeric water are given in parentheses)

Mode	$H_2O \cdot O_3$	$D_2O \cdot O_3$	$HDO \cdot O_3$
	Results of Shriver et al.[49]		
$\nu_1(H_2O)$	3632.5	2654	2697
$\nu_2(H_2O)$	1592.5	1176.5	1399
$\nu_3(H_2O)$	3726.5	2765.5	3691
	Results of Jaeger[52]		
$\nu_1(H_2O)$	3632.15(−5.85)	2652.98(−4.72)	2695.24(−14.86)
$\nu_2(H_2O)$	1593.20(4.10)	1177.18(2.58)	1396.50(−2.3)
$\nu_3(H_2O)$	3726.95(−7.35)	2764.95(−6.15)	3690.98(3.68)

spectroscopy (see also Figures 7,8 and Table 1). The shifts observed for water modes upon complexation indicate that a very weak hydrogen bond was formed. Photolysis of water/ozone/Ar samples has led to two processes: 1) production of hydrogen peroxide and its different isotopic forms at the expense of the water–ozone complex. The decay of the precursor
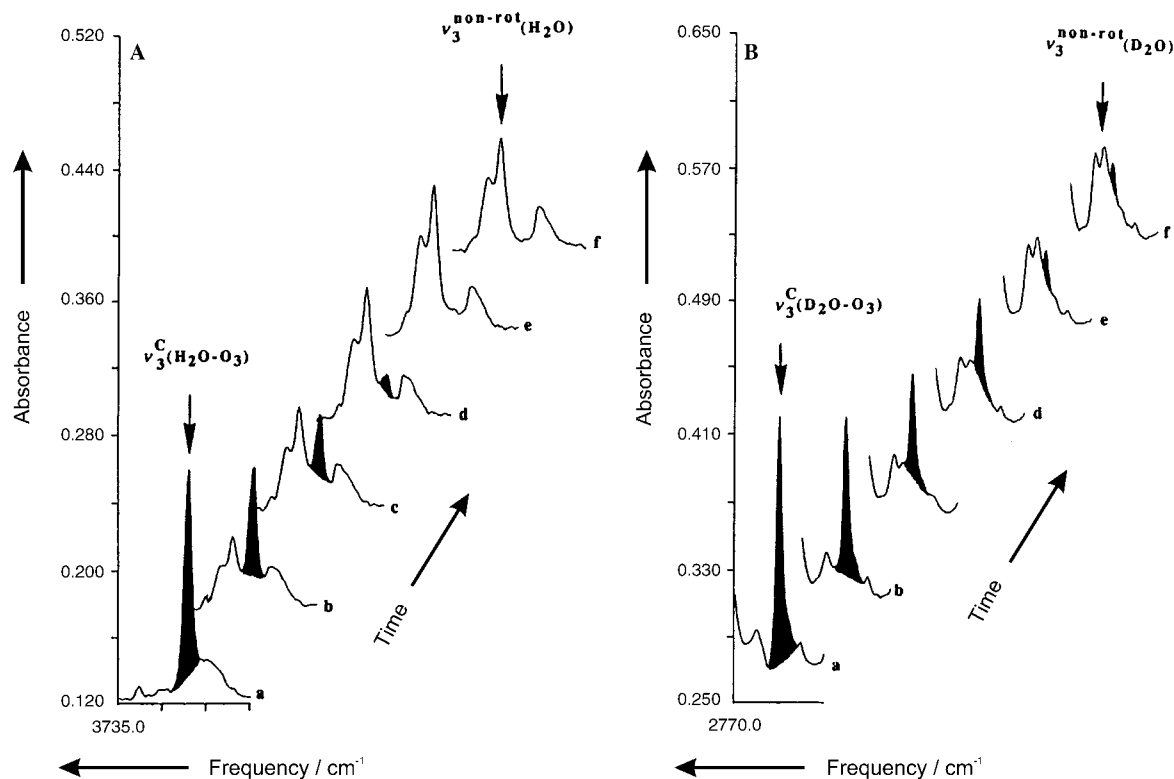
Figure 7. FTIR spectra in the ν_3 and ν_1 regions of a $H_2O \cdot O_3$ complex isolated in an argon matrix (upper trace) and H_2O in an argon matrix for comparison (lower trace). (Reproduced with permission from ref. [52])

$H_2O \cdot O_3$ complex is a first-order reaction. 2) An increase in the amount of nonrotating water monomers due to changes in the matrix structure.

The altitude-dependent concentration profile for the $O_3 \cdot H_2O$ complex in the atmosphere was calculated by Vaida and Headrick.[2] It is significantly different from the profile of the $O_2 \cdot H_2O$ considered above. It is explained, above all, by the significant differences between the concentration profiles, on the one hand, of free dioxygen and ozone, and, on the other hand, of water and ozone. The molar fraction of ozone in the stratosphere is remarkably higher than it is close to the Earth's surface, achieving a maximum of about 10 ppm (altitude range 25–30 km).[53,54] The formation of ozone in the stratosphere is described by Equations (1) and (2).[10,31]

In the upper stratosphere, the source of $O(^3P)$ atoms is the photolysis of dioxygen under UV irradiation at wavelengths lower than 242 nm. In the lower layers of the stratosphere and in the troposphere, where only solar UV irradiation with wavelengths > 290 nm penetrate, the main source of $O(^3P)$—and thus of ozone—is the photolysis of NO_2 ($\lambda < 420$ nm).[10] The abundance of NO_2 in the atmosphere is orders of magnitude lower than the abundance of oxygen. Therefore, the concentration of ozone in the troposphere is significantly lower than in the stratosphere.

In the troposphere, the concentration of H_2O determines not only the concentration of the $H_2O \cdot O_3$ complex but also its concentration profile. Up to an altitude of 10 km, the molar fraction of $H_2O \cdot O_3$, as well as of water vapor, decreases with al-

Figure 8. FTIR spectra in the ν_3 and ν_1 regions of a $H_2O \cdot O_3$ complex (A). The complex band is marked black and decreases upon UV photolysis (spectra b–f). FTIR spectra in the ν_3 and ν_1 regions of $D_2O \cdot O_3$ complex (B). The complex band is marked black and decreases upon UV photolysis (spectra b–f). (Reproduced with permission from ref. [52])

titude. In this region, the increase in the ozone concentration is high enough to partially compensate for the decrease in water abundance. In contrast, the nonvarying abundance of dioxygen and decreasing concentration of water with altitude results in a decreasing concentration of the $H_2O \cdot O_2$ complex with increasing altitude. Therefore, the molar fraction of $H_2O \cdot O_2$ decreases with altitude more strongly than does the molar fraction of $H_2O \cdot O_3$ in the troposphere (see Figure 2). In the lower stratosphere, the concentration of the $H_2O \cdot O_3$ complex increases up to an altitude of about 25 km. This is again connected to the ozone concentration increase. The concentration profiles of both free ozone and its complex with water show similar trends at an altitude of about 20 km.

As indicated in the Introduction, an important question in atmospheric chemistry is the interaction of atmospheric trace gases with the ensembles of H_2O molecules at ice surfaces. The interaction of ozone with ice films of amorphous and crystalline structure has been studied by FTIR spectroscopy under high vacuum conditions by Chaabouni et al.[55] It was shown that ozone deposited on the ice could exist in two states: physically adsorbed ($O_3 \alpha$) and chemically adsorbed ($O_3 \beta$). $O_3 \beta$ is characteristic only for amorphous ice. The IR spectrum of the ($O_3 \beta$)-form at 55 K shows two IR bands at 3641.0 cm^{-1} in the region of ν_{OH} vibrations of water and at 1033.8 cm^{-1} in the region of the ν_3 ozone band. The first band is near the band at 3620 cm^{-1} in the IR spectrum of the ozone–water complex observed in a low-temperature argon matrix with an excess of water relative to ozone. The second band is the 7 cm^{-1}-shifted ν_3 band of solid ozone. These spectral features are evidence for the interaction between ozone and the hydrated surface of micropores by means of H-bonds at 55 K. In contrast, the α-form of ozone is not sensitive to the presence of OH groups on the ice surface. The intermolecular interaction of O_3 with the smooth, neat ice surface can be characterized as a van der Waals type interaction, analogous to the observations in an ultrasonic jet.[47]

Experimental and theoretical investigations of ozone adsorption on an amorphous ice film have been performed using periodic Hartree–Fock calculations.[56,57] The ice model was an infinite slab with hexagonal symmetry of unit cell of ice *Ih* with different adsorption sites at the surface: dangling hydrogen atoms, dangling oxygen atoms, and four-coordinated water molecules. It was demonstrated that, in this case, the weak interaction of ozone can be of different origin: the nonspecific (electrostatic) interaction between the oxygen atom of the water molecule and the central atom of ozone with a theoretical adsorption energy $\Delta E_a = -15$ kJ mol^{-1} (in good agreement with the experimental desorption energy $E_d = 20 \pm 3$ kJ mol^{-1}), and the specific interaction between the dangling OH group of the surface water molecule and the terminal oxygen atom of ozone. The confirmation of this result is a red-shift of the OH band at 3695 cm^{-1}, characteristic both for the outer ice surface and for the surface micropores. This frequency shift was estimated theoretically to be 80 cm^{-1} which is in reasonable agreement with the experimental value of 60 cm^{-1}. The structure of the adsorption complex of ozone is shown in Figure 9.

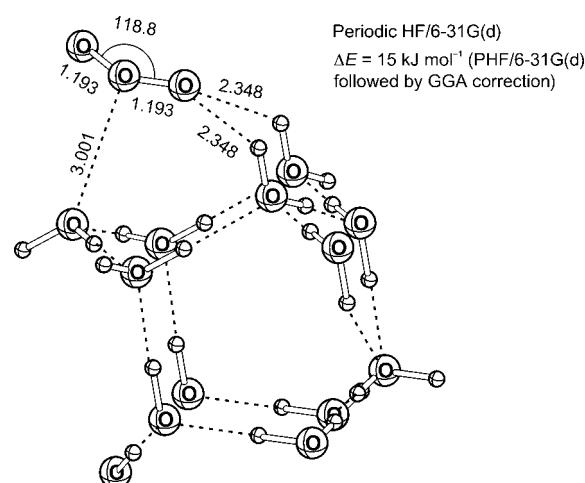*Figure 9.* Structure of the adsorption complex of ozone on an ice surface.[56]

2.4. Complexes of H_2O with Radicals (HO•, HOO•, HOOO•)

The photochemical processes in the ozone–water system are of special interest for at least two reasons. First, weak atmospheric complexes can play a significant role, even when their concentration and, hence, their ability to absorb solar radiation is small.[2, 25, 58–60] They cannot remarkably affect the radiation balance of the atmosphere. However, the reactions of the complexes induced by sunlight can have a remarkable effect on the formation of photochemically active radicals in the atmosphere. In particular, although the atmospheric concentration of the $H_2O \cdot O_3$ complex is low, the atmospheric production of HO• radicals can be significantly influenced by its photolysis.[58, 59, 61] This fact is especially important for the crepuscular periods, when only the low-energy part of the solar spectrum interacts with the red-shifted band of the complex.
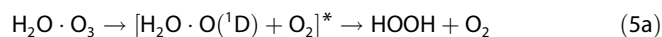
It has been shown that the chemical lifetime of ozone in the Earth's troposphere is very long, both for pure gas-phase conditions and for ozone deposited on ice.[62–65] For example, the lifetime of ozone undergoing thermal destruction at an ice surface has been estimated to be about fifteen years under conditions close to those in the upper troposphere (temperature 223 K–258 K and pressure range 10^{-3}-10^{-1} Pa). Thus, photochemical processes are necessary for the destruction of ozone sticking to ice surfaces.

A detailed study of photochemical transformations of $H_2O \cdot O_3$ in a low-temperature argon matrix has been made.[48][62–65] It has been shown that irradiating the system $O_3/H_2O/Ar$ (concentration ratio $\approx 6/1/600$) with the full spectrum of a xenon lamp results in new IR bands at 3588, 1275, and 1270 cm^{-1} which were assigned to the ν_1, ν_2, and ν_6 vibrations of hydrogen peroxide in solid argon (see ref. [66] for vibration bands of isolated H_2O_2). During the long irradiation, two new bands at 3452 and 3414 cm^{-1} appeared, which are evidence for the formation of a small number of HO radicals.[67–69] Shriver et al.[48, 49] propose that, of the two possible reactions, Equations (4) and (5), Equation (5) has the higher probability, that is, the photolysis is a first-order reaction of the ozone–water com-

plex with a rate constant of $0.20 \pm 0.05 \, \mathrm{hour^{-1}}$ under the given conditions.

$$H_2O + O(^1D) \rightarrow H_2O_2 \tag{4}$$

$$H_2O \cdot O_3 + h\nu \rightarrow H_2O_2 + O_2 \tag{5}$$

The mechanism can be described by Equation (5 a)

$$H_2O \cdot O_3 \rightarrow [H_2O \cdot O(^1D) + O_2]^* \rightarrow HOOH + O_2 \tag{5a}$$

The photolysis of $H_2O \cdot O_3$ in an argon matrix has been studied by Jaeger.[52] Hydrogen peroxide was also found as a basic product. However, the rate constant of Equation (5) was found to be much higher: $0.87 \pm 0.2 \, \mathrm{hour^{-1}}$. This can mean that, under different irradiation conditions, the destruction of the complex and the formation of hydrogen peroxide occurs faster than previously observed.[48,49] It has also been found that the number of the nonrotating water molecules increases over the course of photolysis due to changes in the matrix structure by oxygen atoms and molecules formed during the photolysis.[52]

A study of the photolysis of ozone adsorbed on ice has an important theoretical and practical relevance because this kind of reaction can be realized under the atmospheric conditions during the formation of ice particles of cirrus clouds and polar stratospheric clouds. It is known[14] that reactions occurring on the crystalline ice surfaces of these clouds can be characterized by thermodynamic and kinetic parameters other than under gas-phase conditions. In the case of ozone photolysis on ice surfaces, the stabilization and accumulation of the photolysis products and/or intermediates—the above-mentioned radicals and molecular oxidants—can take place. In an early work,[70] the photolysis of neat solid ozone and ozone in an ice environment was studied.

At a wavelength of 308 nm, the two spin-allowed pathways presenting the primary reactions of the ozone photolysis in the gas phase are given by Equations (6a) and (6b) [compare these with Equation (1)]

$$O_3 + h\nu \rightarrow O(^3P) + O_2(^3\Sigma_g^-) \tag{6a}$$

$$O_3 + h\nu \rightarrow O(^1D) + O_2(^1\Delta_g) \tag{6b}$$

The oxygen atom can react with another ozone molecule and form two oxygen molecules. In the solid phase, it is believed that only the $O(^1D)$ atom reacts with the neighboring ozone molecules, Equation (7a):

$$O(^1D) + O_3 \rightarrow 2O_2 \tag{7a}$$

The most probable behavior of the $O(^3P)$ atom is its recombination with O_2, forming the ozone molecule, Equation (7b):

$$O(^3P) + O_2 \rightarrow O_3 \tag{7b}$$

An important aspect of ozone chemistry is the reaction of O-(^1D) atoms in the gas phase. Two OH radicals can be formed in

this reaction, Equation (8)

$$O(^1D) + H_2O \rightarrow HO^\cdot + HO^\cdot \tag{8}$$

In the solid phase, they recombine forming a hydrogen peroxide molecule, Equation (9)

$$HO^\cdot + HO^\cdot \rightarrow HOOH \tag{9}$$

Simultaneously, Equations (10a) and (10b), can occur

$$HO^\cdot + O(^1D) \rightarrow HOO^\cdot \tag{10a}$$

$$HO^\cdot + O_3 \rightarrow HOO^\cdot + O_2 \tag{10b}$$

forming another oxidant molecule—the peroxy radical. It has been shown[33] that the IR bands at 1405 and 2860 $\mathrm{cm^{-1}}$ did appear in the IR spectrum during the photolysis of solid samples O_3/H_2O. These bands are assigned[66,71,72] to the bending mode and the $\nu_2 + \nu_6$ combination band of hydrogen peroxide, respectively. The quantum yield of the photodissociation of ozone on the ice (0.4 ± 0.2) is lower than in the gas phase (1.5 ± 0.2) where the chain reactions of the $HO^\cdot$ radicals occur.

The formation of hydrogen peroxide as a basic product of ozone photolysis on an ice surface was confirmed recently by reflection–adsorption IR spectroscopy at 80 K.[33] The reflection–absorption FTIR (RAFTIR) spectrum of $O_3 \cdot H_2O$ mixtures deposited on a cold metallic surface at 80 K was registered before and after UV irradiation at 250 and 320 nm. The irradiation resulted in remarkable changes in the IR spectrum. The absorption bands of the ozone molecules disappeared completely, whereas two new bands appeared: an intense band at 2860 $\mathrm{cm^{-1}}$ and a broad band at 1450 $\mathrm{cm^{-1}}$ of low intensity. Moreover, a remarkable reshaping of the broad bands at 3100–3600 and 500–1000 $\mathrm{cm^{-1}}$ took place. The subsequent annealing of the irradiated films up to 203.2 K had only a small effect on the IR spectra: The band at 2860 $\mathrm{cm^{-1}}$ was slightly sharpened, and shifted to 2855 $\mathrm{cm^{-1}}$, without any change in peak intensity. In the case of the band at 1450 $\mathrm{cm^{-1}}$, a low-intensity satellite band at 1390 $\mathrm{cm^{-1}}$ appeared. In addition, a low-intensity feature appeared at 1100 $\mathrm{cm^{-1}}$. Among these bands, the band at 2860 $\mathrm{cm^{-1}}$ was assigned to the $\nu_2 + \nu_6$ combination band of H_2O_2, although the DFT study also points out the possible small admixture of the IR vibrations of adsorption complexes between the ice surface and the $HOO^\cdot$ and $O(^1D)$ formed in the course of ozone photolysis at the ice surface.

Photolysis of O_3 to produce $O(^1D)$ is currently thought to be the main contributor to the atmospheric production of hydroxyl radicals, see Equation (8). It is worthwhile to note that another possible source of hydroxyl radicals in the troposphere, the photolysis of the above-described ozone–water weakly bound complex [Equation (11)], has been investigated[61]
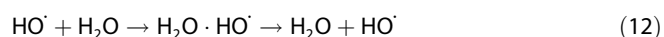
$$H_2O \cdot O_3 + h\nu \rightarrow 2HO^\cdot + O_2 \tag{11}$$

The calculated production of $HO^\cdot$ from $H_2O \cdot O_3$ photolysis at the Earth's surface ranges from 1% to 15% of the lowest measured daytime $HO^\cdot$ production rates in the troposphere. The

contribution of the complex to HO• production probably decreases with increasing altitude. Assuming the calculated rate constant of the complex $H_2O \cdot O_3$ photolysis and its electronic binding energy to be 10.0 kJ mol^{-1}, Frost and Vaida[61] estimated a five-fold reduction in the relative contribution of $H_2O \cdot O_3$ between the surface and 15 km altitude. A combined analysis of both channels of formation of HO• [bimolecular, Equation (8), and via the complex, Equation (11)], has shown that the calculated production of HO• from the photolysis of $O_3 \cdot H_2O$ complexes could represent a significant source of HO• in the troposphere.

The hydroxyl radical can also react with water, a complex is the intermediate of this reaction, Equation (12)

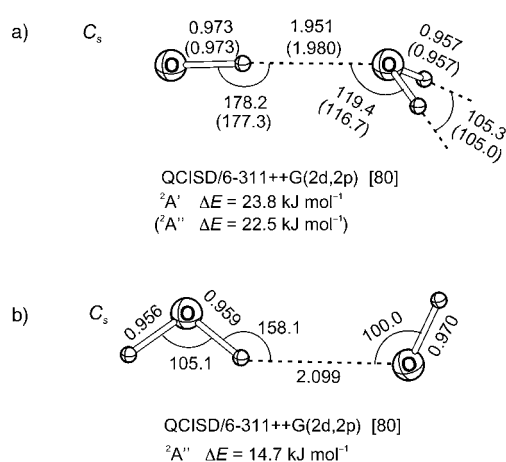$$HO• + H_2O \rightarrow H_2O \cdot HO• \rightarrow H_2O + HO• \qquad (12)$$

Taking into account the importance of the interaction of hydroxyl radicals with water, several theoretical studies of the ground state of the $H_2O \cdot HO$ complex have been made over the past decade.[73–81] It was recognized in an early study[73] that $H_2O \cdot HO•$ is characterized by C_s symmetry and that it has two low-lying electronic states of $^2A'$ and $^2A''$ symmetry originating from two doubly degenerate $^2\Pi$ states of OH•. When HO• approaches a water molecule, the $C_{\infty v}$ point group of the HO• radical is reduced to the C_s symmetry of the complex, and the two degenerate components of the $^2\Pi$ states split into the distinct $^2A'$ and $^2A''$ states of the complex. These states are distinguished by the position of the highest occupied molecular orbital (HOMO), which can be located *in* ($^2A'$) or *out* of the symmetry plane ($^2A''$). Moreover, the hydroxyl radical may form a hydrogen bond to H_2O through either the oxygen or the hydrogen atom. Kim et al.[73] used the RHF, UMP2, UCISD, and RCISD methods with the STO-3G, DZ, DZP, and TZ2P basis sets to treat the former case, finding two minima belonging to the C_s point group with $^2A''$ and $^2A'$ symmetry. The HO• radical in these structures is a donor of electronic density, that is, a hydrogen bond is formed between the oxygen atom of OH and the hydrogen atom of H_2O (this structure is similar to the one shown in Figure 10 b). In a further and more detailed study, Xie

and Schaefer[74] used HF and CISD theories and the DZP and TZ2P basis sets. They found that HO• can be bound not only through the hydrogen atom of water but also through the hydrogen atom of the radical, forming a bent structure with C_s symmetry, where HO• is an acceptor of electronic density (similar to the structure shown in Figure 10 a). Additionally, a planar HO-accepting structure with C_{2v} symmetry was considered. In all the structures, the two lowest $^2A'$ and $^2A''$ electronic states ($^2B_1$ and $^2B_2$ in the case of C_{2v} structures) were examined.[74] It was found that the global minimum corresponds to the HO-acceptor structure with C_s symmetry in the $^2A'$ electronic state, with a binding energy of 23.8 kJ mol^{-1}. The $^2A''$ state lies only 1.3 kJ mol^{-1} higher ($\Delta E = 14.6$ kJ mol^{-1}) and is only slightly different in geometry. The binding energies of HO-donor structures are 14.6 kJ mol^{-1} ($^2A''$) and 9.5 kJ mol^{-1} ($^2A'$). Later, density functional calculations by Wang et al.[75] showed that the HO-acceptor structure $^2A'$ (but not $^2A''$) considered by Xie and Schaefer[74] is not a true minimum (it has an imaginary vibrational frequency corresponding to the out-of-plane distortion). Similarly, the planar C_{2v} HO-acceptor conformations (both $^2A'$ and $^2A''$) are the transition states between two bent structures of C_s symmetry. Recently, Langford et al.[76] and Cooper et al.[77] reexamined these possible conformations of this complex using higher levels of theory. It was found[77] that, in agreement with results reported by Xie and Schafer and Wang et al.,[74,75] the global minimum at the QCISD/6-311++G(2d,2p) level is an HO-acceptor complex of $^2A'$ symmetry with a binding energy of 23.8 kJ mol^{-1}. The next-lowest HO-acceptor minimum ($^2A''$) is a similar structure with a ΔE of 22.5 kJ mol^{-1}. The stable HO-donor structure ($^2A''$) has a significantly lower binding energy of 14.7 kJ mol^{-1}. Figure 10 shows the geometry structures and the optimized geometry parameters of the true minima of the $H_2O \cdot HO•$ complex. Since, in the paper of Cooper et al.,[77] the optimized geometry parameters were not indicated in the figures, Figure 10 shows the geometry parameters, which were recalculated by us at the same level of theory.

It should be noted that in a most recent work,[78] the planar conformation of the $H_2O \cdot HO•$ and the HO-acceptor $^2A'$ state (optimized at the SCF level) were considered as stable forms and an analysis of the experimental data (assignments of IR absorption bands in an inert matrix) was performed on this basis. The stability of the planar and HO-acceptor ($^2A'$) conformations is probably a result of the lack of electronic correlation, which can also explain the results of Xie and Schaefer.[74]

The experimental identification and assignment of absorption bands of the $H_2O \cdot HO•$ complex in the IR spectrum of HO• embedded in argon matrices (11.5 K, H_2O:Ar ratios from 1:70–1:1000) was carried out by Langford et al.[76] These authors assigned the bands at 3452 and 3428 cm^{-1} to the $H_2O \cdot HO•$ complex occupying two sites in the argon matrix. This assignment is in agreement with theoretical predictions of the red-shift of the OH stretching bands upon complexation, and gives a good account of the experimental results obtained here and by other workers. At the same time, it was stated that further work is required to confirm this assignment. In particular, the most convincing evidence for the existence of the $H_2O \cdot HO•$

a) C_s

0.973
(0.973)   1.951
(1.980)   0.957
(0.957)

178.2
(177.3)   119.4
(116.7)   105.3
(105.0)

QCISD/6-311++G(2d,2p) [80]
$^2A'$ $\Delta E = 23.8$ kJ mol^{-1}
($^2A''$ $\Delta E = 22.5$ kJ mol^{-1})

b) C_s

0.956   0.959   158.1   100.0   0.970

105.1   2.099

QCISD/6-311++G(2d,2p) [80]
$^2A''$ $\Delta E = 14.7$ kJ mol^{-1}

Figure 10. *Stable structures of the complexes of the HO radical with water. a) HO-acceptor (A′ and A″ electronic states); b) HO-donor (A″ electronic state).*

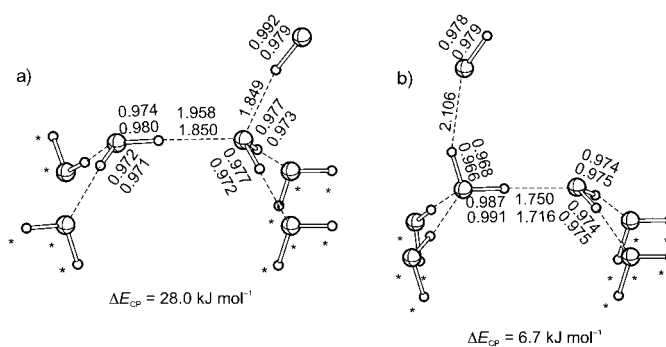complex could be found between 400 and 650 cm^{-1} in the $H_2O \cdot HO^\bullet$ torsion (a'') and H···OH bending regions, where these authors were unable to acquire data at present. Langford et al.[76] found no significant shift of the band frequencies corresponding to the water part of the complex. This is not unexpected, if water acts as a hydrogen bond acceptor in the complex. The fundamental frequencies of the coordinated water should therefore appear very close to those of the water monomer, and may mask weak complex bands. In order to avoid excessive water concentrations in their matrix isolation study of the $H_2O \cdot HO^\bullet$ complex, Engdahl et al.[78] co-deposited peroxy radicals and molecular hydrogen in argon matrices and then generated the HO$^\bullet$ water complex directly by UV radiation. In this way, they were able (for the first time) to observe the coordinated water. A band at 3453.5 cm^{-1} of a coordinated HO$^\bullet$ radical appeared simultaneously with the bands of a water molecule which accepts a hydrogen bond from another molecule. It was also concluded that the complex is effectively planar with the OH radical rotating around the C_2 axis of water.[78] This observation is clearly compatible with the assumption that a peroxy radical, trapped together with a hydrogen molecule, transforms into a water–hydroxyl radical complex after absorbing a 266 nm photon. The only water complexes that have been observed to rotate around the C_2 axis of water are the hydrogen halide and diatomic halogen complexes. That is the basis for confidence that the hydrogen bond donor to the observed hydrogen bond acceptor is a linear molecule. Consequently, hydroxyl radicals form a hydrogen bond to a water molecule and the complex is effectively planar, allowing free rotation around the C_2 axis of water. However, it does not agree with the complex shift (approximately 100 cm^{-1}) of OH forming a hydrogen bond to water. That is very close to the complex shift of HDO (102 cm^{-1}), which forms a H-bond to another water molecule.[79] The authors explain this fact by different contributions of zero point vibrational energies to the total binding energy in both complexes.

Cooper et al.[77] have reexamined the infrared spectrum of the $H_2O \cdot HO^\bullet$ complex in argon matrices at 11.5 ± 0.5 K and calculated the vibrational frequencies and band intensities of the complex. As a result of these measurements and calculations, a previously unassigned absorption band at 3442.1 cm^{-1} was assigned to the OH stretch in the OH radical bound to the water molecule. This absorption originates from a complex that is located in a different site within the argon matrix to those absorptions already assigned to this vibration at 3452.2 and 3428.0 cm^{-1}. A decrease in the intensity of the OH radical stretching vibration of the $H_2O \cdot HO^\bullet$ complex upon isotopic substitution of deuterium for hydrogen was observed. This result agrees well with the conclusion that the HO-acceptor form is the most favorable conformation of $H_2O \cdot HO^\bullet$.

In summary, one can state that the experimental results for this system are somewhat controversial. However, on the basis of the results obtained at the highest level of theory and the most recent experimental results,[77,78] we conclude that the $H_2O \cdot HO^\bullet$ complex is an HO-acceptor system with a structure close to that shown in Figure 10a. The observed IR frequencies of the $H_2O \cdot HO^\bullet$ complex are summarized in Table 2.

Table 2. Observed IR absorption bands of the OH radical in the hydroxyl–water complex [cm^{-1}] isolated in an argon matrix (the corresponding values for $D_2O \cdot DO^\bullet$ are given in parentheses).

Assignment	Observed band [76]	Observed band [77]	Observed band [78]
HO	3549.6		
HO	3548.1		
$H_2O \cdot HO$, site 1	3452.2	3452.2 (2542.9)	3453.5 (2543.6)
$H_2O \cdot HO$, site 2		3428.0 (2524.6)	
$H_2O \cdot HO$, site 3	3428	3442.1 (2534.6)	

Figure 11. Structure of the complex of HO$^\bullet$ with an ice cluster: a) HO-donor structure; b) HO-acceptor structure. The lower values are the bond lengths of an undistorted cluster. Asterisks mark the atoms fixed in the optimization. Optimization was at the B3LYP/6-31++G(d,p) level, energy calculations at B3LYP/6-311++G(2d,2p)/B3LYP/6-31++G(d,p).[33]

The formation of complexes between HO$^\bullet$ radicals and ice-like water clusters has been modeled by Ignatov et al.[33] It was shown that HO$^\bullet$ can interact with either dangling hydrogen or oxygen atoms (analogously to HO-donor or HO-acceptor structures of the binary complex $H_2O \cdot HO^\bullet$). The geometry optimization results in two stable structures with one-fold HO$^\bullet$ coordination on the terminal oxygen or hydrogen atoms (Figure 11). The coordination of HO$^\bullet$ does not result in breaking a surface H-bond. The corresponding binding energy of the most favorable complex (HO-donor) is 30.1 kJ mol^{-1} ($\Delta E_{CP} = 28.0$ kJ mol^{-1}) which is significantly higher than in the binary complex $H_2O \cdot HO^\bullet$ (23.8 kJ mol^{-1}). The HO-acceptor structure has only 7.5 kJ mol^{-1} ($\Delta E_{CP} = 6.7$ kJ mol^{-1}) in comparison with 14.7 kJ mol^{-1} of the binary complex. The OH bond in the OH-donor complex is remarkably elongated: $r(O-H) = 0.992$ Å (0.979 Å in the isolated radical). However, the calculated vibrational frequencies are quite close to the frequencies of the initial cluster. It should be noted that the absorption band of the OH bond of the radical is located in the region of 3400–3500 cm^{-1}, in the middle of the OH band of the cluster and, thus, is masked by the broad OH-band of clustered H_2O molecules.

In a study by Nelander,[82] a water complex with one of the very reactive participants in the gas-phase chemistry of the troposphere (where the water concentration is high) and in the stratosphere (at low temperatures)—the peroxy radical HOO$^\bullet$—was investigated. It was proposed on the basis of other laboratory studies[83–86] that the formation of the $H_2O \cdot HOO^\bullet$ complex
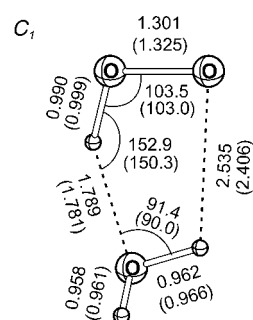
can speed up the formation of hydrogen peroxide by a factor of three.

Nelander[82] reported that the most effective method for peroxy radical synthesis in a low-temperature matrix is the addition of a hydrogen atom to molecular oxygen. When the HOO• radical and water were present in the matrix simultaneously, significant changes were observed in the IR spectrum in comparison with the spectra of the individual components (Table 3).

Table 3. *Observed IR absorption bands of the peroxy–water complex [cm^{-1}] isolated in an argon matrix.*[82]

Vibration mode	Uncoordinated H_2O + HOO•	HOH·OOH Complex
$\nu_1(H_2O)$	3638.0	3501.5
$\nu_3(H_2O)$	3734.3	3691
$\nu_1(HOO)$	3413.0	3236.2
$\nu_2(HOO)$	1388.9	1479.3
$\nu_3(HOO)$	1100.8	1120.4
$2\nu_2(HOO)$		2875
		2858
		2833

The remarkable red-shift for the valence bands and the blue-shift for the deformation bands of the peroxy radical and the simultaneous red-shift of the valence bands of water in the complex indicate that both molecules act as proton donors. Thus, the complex should be characterized by a cyclic structure with the peroxy unit having the hydrogen atom oriented towards the oxygen atom of water. The water hydrogen atoms, in turn, form hydrogen bonds with the terminal oxygen atom of the radical. Such a structure is similar to the structure of the water trimer. The binding energy of the complex, estimated on the basis of a comparison of the experimental shift for the OH vibrations of water with the analogous values for the known complexes, is about 25 kJ mol^{-1}. These results show that the peroxy radical is more acidic in character than water and readily forms hydrogen bonds. Therefore, its water affinity (solubility) should be high. The experiments on the uptake of peroxy radicals by liquid water (studied in a flow tube reactor with wetted walls) give much higher values of the absorption and Henry's coefficients than takes place for water and, thus, support this proposal.[87]

The results of Nelander's experimental study[82] are in good agreement with quantum chemical calculations.[88–91] Among the theoretical works, it is believed that the most reliable results are those of Aloisio and Francisco,[90] where calculations were carried out at the MP2/6-311++G(2df,2p) level of theory, and those of Aloisio et al.[91] (calculations of the excitation energies of the three lowest electronic states of HOO• and H_2O·HOO• using CASSCF and MRCI methods). It was found that the most favorable conformation of the complex is an asymmetric five-membered cyclic structure [···O(H)—H···O—O—H···] with one of the water hydrogen atoms located out of the molecular plane (Figure 12). At the best levels of theory [MP2/6-311++G(2df,2p) and B3LYP/6-311++G(3df,2pd)], the O$_{water}$···

UMP2/6-311++G(2df,2p)   [93]
ΔE = 40.2 kJ mol^{-1}

(B3LYP/6-311++G(3df,3pd) [93])
(ΔE = 36.8 kJ mol^{-1})

Figure 12. *Structure of the H_2O·HOO• complex.*

H$_{radical}$ hydrogen bond lengths are, correspondingly, 1.789 and 1.781 Å, whereas the O$_{radical}$···H$_{water}$ bonds are significantly longer: 2.535 and 2.406 Å. The best estimate of the BSSE-corrected binding energy obtained at the CCSD(T)/6-311++G(2df,2p)//B3LYP/6-311++G(2df,2p) level is 39.3 kJ mol^{-1}. The ZPE-corrected value D_0 = 28.9 kJ mol^{-1}. The D_0 value is in agreement with the binding energy of the complex proposed on the basis of an FTIR argon matrix study of this complex[82] estimated to be 25 kJ mol^{-1}.

The observed vibrational frequencies of the complex at 3236.2, 1479.3, and 1120.4 cm^{-1} (see Table 3) are in good agreement with the calculated values. Aloisio et al.[90] also estimated the concentration of the H_2O·HOO• complex in the atmosphere. It is expected that the highest concentration of this complex exists in the lower atmospheric regions, where the highest concentration of water is observed.

Aloisio et al.[92] have also experimentally studied the formation of the complex of HOO• with H_2O using a discharge flow cell by FTIR spectroscopy. These studies [Equation (13)] were carried out between 230 and 298 K in the presence of excess H_2O.

$$HOO^{\bullet} + H_2O \leftrightarrow H_2O \cdot HOO^{\bullet} \qquad (13)$$
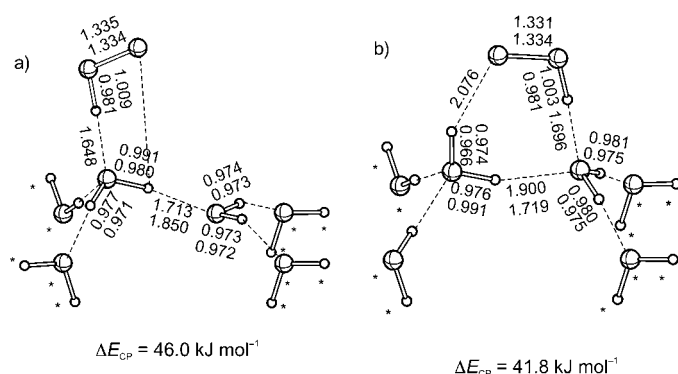
On the basis of measurements of the HOO• disappearance, equilibrium constants (K_c) for the formation of the complex are 1.7×10^{-16}, 4.1×10^{-17}, and 4×10^{-18} cm^3 molecule^{-1} at 230, 250, and 298 K, respectively. The enthalpy of complex formation is -36 ± 16 kJ mol^{-1}. A value of -85 ± 40 J mol$^-$ K^{-1} was calculated for the reaction entropy. This is in good agreement with previous estimates made from kinetic measurements[93] and theoretical calculations.[88] The relative stability of the complex, coupled with the presence of large ambient concentrations of H_2O, implies that H_2O·HOO• may coexist with free HOO• in the Earth's atmosphere. Both the atmospheric water vapor concentration and the equilibrium constant of Equation (13) strongly depend on the altitude, varying, however, in opposite directions. On one hand, the concentration of H_2O decreases from

approximately 3×10^{17} molecule cm^{-3} near the surface to 2×10^{13} molecule cm^{-3} at the tropopause. On the other hand, the equilibrium constant increases from approximately 2×10^{-18} cm^3 molecule^{-1} near the surface to 1×10^{-15} cm^3 molecule^{-1} at the tropopause. Convolution of these parameters favors the formation of the $H_2O \cdot HOO^\bullet$ complex at altitudes between 1 and 3 km. In that altitude range, $H_2O \cdot HOO^\bullet$ levels may rise to up to 30% of the $HOO^\bullet$ levels. Because of the fast chemical coupling between HO_2 and H_2O, Equation (13), it seems probable that $H_2O \cdot HOO^\bullet$ plays a role as the temporary reservoir of $HOO^\bullet$ in the atmosphere.

The interaction of $HOO^\bullet$ with an icelike water cluster was theoretically studied by Ignatov et al.[33] The geometry optimization of the cluster with adsorbed $HOO^\bullet$ shows that the radical does not break the surface hydrogen bond. It can only form the onefold coordinated complex with both kinds of the surface bond oxygen atoms (see Figure 13). The $O \cdots HOO^\bullet$ com-

Figure 13. *Structure of a complex of HO with ice clusters: a) onefold coordinated structure; b) twofold coordinated structure. The lower values are the bond lengths of an undistorted cluster. Asterisks mark the atoms fixed in the optimization. Optimization at the B3LYP/6-31++G(d,p)level, energy calculations at B3LYP/6-311++G(2d,2p)/B3LYP/6-31++G(d,p).[33]*
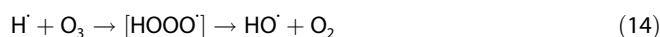
plex with a terminal oxygen has a binding energy of 33.9 kJ mol^{-1}. The more stable structure is formed when $HOO^\bullet$ interacts with the opposite oxygen atom of the surface hydrogen bond. The binding energy of this complex is 54.3 kJ mol^{-1}. The $r(O–H)$ distance of the coordinated peroxy radical is sufficiently increased compared to the free molecule: $r(OH) = 1.009$ Å (0.981 Å in isolated $HOO^\bullet$). This results in a significant decrease in the frequency of the OH group valence vibration of the adsorbed $HOO^\bullet$, to 3105 cm^{-1} (scaled value 2950 cm^{-1}), whereas the frequency of the isolated molecule is 3574 cm^{-1} (scaled 3395 cm^{-1}). The complex has an intense peak of $HOO^\bullet$ adsorbed on the surface (2950 cm^{-1}) which is only 90 cm^{-1} higher than the position of the experimentally observed intense band of 2860 cm^{-1}. Thus, it cannot be excluded that the experimentally observed band (assigned to $\nu_2 + \nu_6$) contains an admixture of OH stretching of $HOO^\bullet$.

In very recent studies of the Francisco group,[94, 95] an $(H_2O)_{20}$ spherical cage was used as a model of a cloud droplet. This model was chosen because it is the perfect balance between being large enough to contain an $HOO^\bullet$ radical and small

enough for quantum chemistry optimizations. They found that the interaction of an $HOO^\bullet$ radical with a water surface can be described by a localized interaction picture. Three stable conformations of $(H_2O)_{20} \cdot HOO^\bullet$ were located.[94] The most stable one is a cyclic structure with a $HOO^\bullet$ radical coordinated on two outermost water molecules of the $(H_2O)_{20}$ cluster. In the most stable conformation, $HOO^\bullet$ forms a seven-membered ring [$\cdots H–O–O\cdots H–O(H)\cdots H–O–H\cdots$]. A detailed natural bond orbital (NBO) analysis was performed to elucidate the nature of the strong binding of $HOO^\bullet$ to the cluster.[95] It was found that the two most significant contributions of such a bonding are interactions between: 1) a nonbonding lone pair from the water molecule that is bound to the hydrogen atom of the $HOO^\bullet$ and the σ^*_{OH} antibonding orbital of the $HOO^\bullet$ radical; and 2) a nonbonding electron density of the terminal oxygen atom of the $HOO^\bullet$ and the "in-ring" σ^*_{OH} antibonding orbital of the other water molecule. It was concluded that these interactions are the major forces that account for the sticking of $HOO^\bullet$ to a water molecule. Thus, an important conclusion that can be made on the basis of this study is that the interaction between water clusters and $HOO^\bullet$ and similar radicals has mostly local character (without a strong impact from long-range multipole contributions from the distant parts of a large system) and can be modeled by relatively small clusters. This conclusion is also supported by the fact that the interaction energy is not greatly influenced by the variation of the $(H_2O)_n \cdot HOO^\bullet$ cluster size for $n = 1, 2, 6, 20$.[95]

It should be specially noted that one of the most important questions of modern atmospheric chemistry is the interaction of $HOO^\bullet$ with aerosol particles and droplets in the atmosphere. This process ultimately impacts the ozone and NO_x balance in the troposphere, but is not yet completely understood. Namely, the values of mass accommodation and sticking coefficients of $HOO^\bullet$ on liquid and solid interfaces are highly uncertain, resulting in a large uncertainty in choosing the atmospheric models. Many attempts have been made to estimate the radical–interface interaction parameters using molecular dynamics (MD). The results of MD studies are outside the scope of this review. We refer the interested reader to special works dedicated to this matter: A good, current survey may be found in ref. [96]. A corresponding study of the $H_2O \cdot HOO^\bullet$ potential surface, directed to the elaboration of the effective model potential for MD simulations, can be found in ref. [97].

Aloisio and Francisco[98] have theoretically studied the possibility of forming a complex between water and another unstable radical, HO_3, which can act as metastable radical, Equation (14)

$$H^\bullet + O_3 \rightarrow [HOOO^\bullet] \rightarrow HO^\bullet + O_2 \qquad (14)$$

These calculations show that, by forming a complex with water, HO_3 is stabilized by about 27.2 kJ mol^{-1}, as calculated at the CCSD(T)/6-311++G(2df,2p)//B3LYP/6-311++G(2df,2p) level of theory (Figure 14). It was also shown that the lifetime of the $H_2O \cdot HO_3$ complex may be twenty to five-hundred-times longer than that for the HO_3 monomer under appropriate experimental conditions. This means that water coordination is

c_1
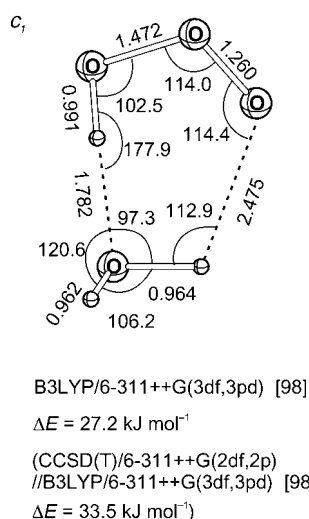

B3LYP/6-311++G(3df,3pd) [98]

ΔE = 27.2 kJ mol^{-1}

(CCSD(T)/6-311++G(2df,2p)
//B3LYP/6-311++G(3df,3pd) [98]

ΔE = 33.5 kJ mol^{-1})

Figure 14. *Structure of the $H_2O \cdot HOOO^\bullet$ complex.*[98]

significant for stabilizing this otherwise metastable molecule. More importantly, the results suggest the possibility that similar metastable molecules may be stabilized by water coordination. Although the effect of this stabilization on atmospheric chemistry is unclear, due to the unknown reactivity of HO_3, Aloisio and Francisco[98] made some speculations. If the water concentration is high and H_2O stabilizes HO_3, the lifetime of the radical is sufficient for it to react with other molecules. A possible reaction consequence of the HO_3 reaction is the transfer of oxygen from HO_3 to a reactant. To provide a competitive reaction rate of this channel in comparison with the dissociation of HO_3, the radical should have a concentration at least of 10^{13} molecule cm^{-3}. No experimental observations on this complex have been reported to date.

2.5. Complexes of H_2O with H_2O_2

The most stable product of ozone photolysis in the presence of water is H_2O_2. It has been shown[34,35] that H_2O_2 is evolved from the photolysis products and the complex $H_2O \cdot O$ is an initial intermediate of this reaction. It has also been demonstrated that the sum of the H_2O_2, $H_2O \cdot O$, and $HO^\bullet$ radical pair concentrations is a constant during the process, which indicates the close nature of the photochemical process [Eq. (15)]

$$H_2O \cdot O \rightleftharpoons H_2O_2 \rightarrow 2HO^\bullet \qquad (15)$$

Hydrogen peroxide can be emitted from the sea to the atmosphere. It can be produced during the synthesis of halogen-containing species in the seawater.[99] As in the case of liquid water, a network of hydrogen bonds is also formed in the case of liquid H_2O_2. Therefore, it can be expected that complexes between H_2O and H_2O_2 molecules can form in the atmosphere. Under laboratory conditions, this complex was observed for the first time in an oxygen matrix.[100] However, a conclusion about the complex structure was not made on the basis of this IR study. Recently, the complex $H_2O \cdot H_2O_2$ was studied in

detail in an argon matrix.[101] It was found that the IR bands of the valence OH vibrations of both H_2O_2 and H_2O units are significantly red-shifted. A comparison of the IR spectral features of the protonated and deuterated species allows the conclusion that the complex is cyclic, where both monomer units are donor and acceptors of hydrogen atoms. Thus, the bifurcated structure, where HOOH forms two hydrogen bonds with the oxygen atom of the water molecule, proposed as the most probable one,[100] should not be considered further. The shift in the OH valence band due to complex formation was very close to the analogous shift in the water trimer. Therefore, it can be proposed that the strength of the H-bond in the complex is close to the strength of the H-bond in the water trimer (14.2 kJ mol^{-1}).[102]

Quantum chemical studies of the complex $H_2O \cdot H_2O_2$ have been performed.[103–105] In the most recent study,[105] MP2 and DFT (with different types of functionals) with various basis sets up to 6-311+G(3df,2p) were used for the investigation. G2-(MP2) theory was applied for the energy improvement. Two different conformations of the complex were considered: the cyclic and open structures. The most stable conformations correspond to the asymmetric cyclic structure of a five-membered ring $\cdots$O(H)—O—H$\cdots$O(H)—O—H$\cdots$ with terminal hydrogen atoms located out of the cycle plane (Figure 15). The most reliable estimate for the BSSE and ZPE-corrected binding energy D_0 is 20.1 kJ mol^{-1} at the G2(MP2) level. The calculated frequencies and the corresponding shifts are in good agreement with those observed.[100,101]
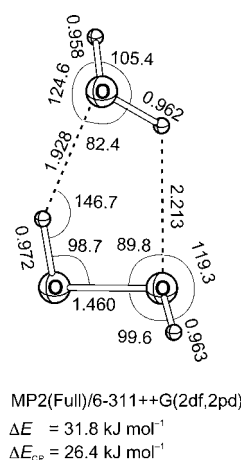

MP2(Full)/6-311++G(2df,2pd)

ΔE = 31.8 kJ mol^{-1}
ΔE_{CP} = 26.4 kJ mol^{-1}

Figure 15. *Structure of the $H_2O \cdot H_2O_2$ complex.*[100]

Very recently, the intermolecular interactions and thermodynamic properties of water–hydrogen peroxide clusters $(H_2O)_n \cdot H_2O_2$, where $n = 1$–3, have been studied by ab initio SCF and Møller–Plesset correlation correction methods employing 6-311G(d) and aug-cc-pVDZ basis sets.[106] It was shown that these clusters form cyclic structures, with both H_2O_2 and H_2O molecules acting as proton donors and proton acceptors, whereas the linear and the bifurcated structures could be located as stable minima on the potential energy surface. The BSSE-corrected binding energies of the stable dimer, trimer, and tetramer were predicted to be -26.1, -54.5, and
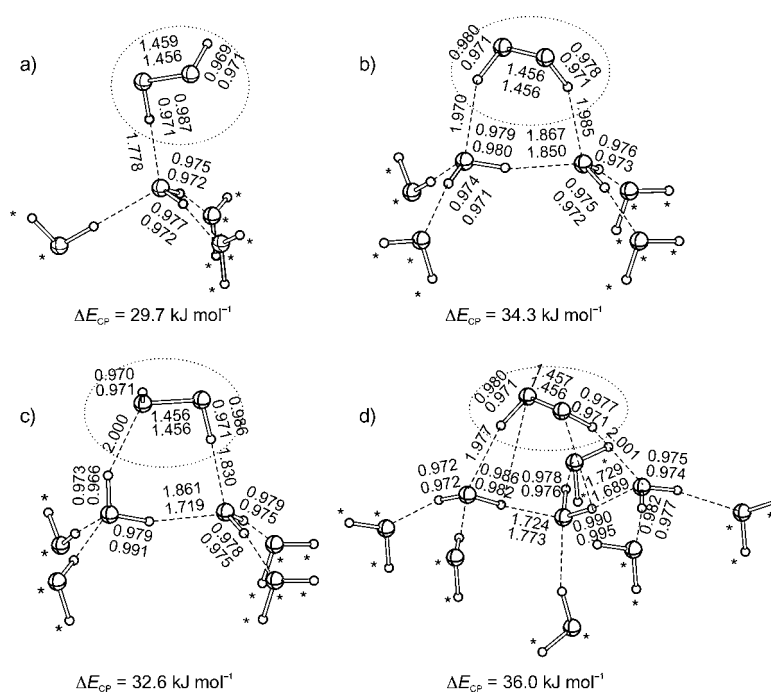
−98.7 kJ mol⁻¹, respectively, at the MP4/aug-cc-pVDZ//MP2/aug-cc-pVDZ level (−28.4, −59.5, and −108.8 kJ mol⁻¹ at the MP2/aug-cc-pVTZ//MP2/aug-cc-pVDZ level). The calculated binding energy for the dimer is in good agreement with the value estimated from the experimental frequency shifts. Because the binding energy of the tetramer is almost as much as quadruple that of dimer, the authors concluded that cooperative effects take place in the trimers and tetramers. The hydrogen bond between H_2O_2 and H_2O, with the former as the proton donor, is stronger than that with H_2O_2 as the proton acceptor in all clusters. The interactions elongate the O—O bonds and decrease the O—O stretching frequencies for all clusters, in agreement with experimental observations. Frequencies associated with the O—H rocking and stretching of

Figure 16. Structure of a complex of H_2O_2 with ice clusters: a) onefold coordinated structure; b) twofold coordinated hydrogen-bonded structure; c) twofold coordinated (O,H)-bonded structure; d) adsorption complex at the basal plane of the ice crystal. The lower values are the bond lengths of an undistorted cluster. Asterisks mark the atoms fixed in the optimization. Optimization at the B3LYP/6-31++G(d,p)level, energy calculation at B3LYP/6-311++G(2d,2p)/B3LYP/6-31++G(d,p).[33]

H_2O_2 in the binary complex are also in good agreement with experiment.

The interaction is an exothermic process and is accompanied by a decrease in entropy. The change in Gibbs free energy for the aggregation from the monomer to the dimer, trimer, and tetramer were predicted to be 10.98, 20.24, and 17.30 kJ mol⁻¹, respectively, under standard conditions.

The uptake of H_2O_2 by an ice surface has been experimentally studied[107] by mass-spectrometry from 213–238 K and over the partial pressure range 10^{-5}–10^{-2} Pa. It was shown that, in contrast with the strong acids (HNO_3 and HCl) and SO_2, the uptake has a reversible character. It is not accompanied by H_2O_2 dissociation, but is controlled by the formation of H-bonds with the surface.

A detailed quantum chemical study of the interaction of H_2O_2 with icelike clusters (modeling the ice surface) has shown that H_2O_2 molecules can interact with an ice surface in different coordination modes.[33] It can form one-, two-, or multi-fold coordination complexes with the dangling OH groups or terminal oxygen atoms at the basal or side planes of the ice crystal: These complexes can be distinguished both in energy and in vibrational frequencies (see Figure 16).

The optimized structure of the one-fold coordination adsorption complex of H_2O_2 is similar to the most stable conformation of a binary complex[101] between H_2O and H_2O_2, both in structure and in energy. The binding energy (36.0 kJ mol⁻¹) is close to the binary complex value at the B3LYP/6-31++G(d,p) level (32.2 kJ mol⁻¹). The frequency calculation shows that the frequency of the lowest OH stretching mode (stretching of the

OH group of the coordinated H_2O_2 molecule) is 3448 cm⁻¹. The scaled value is 3276 cm⁻¹, which is far from the observed band of 2860 cm⁻¹.

The one-fold coordination of an H_2O_2 molecule at the dangling hydrogen site (i.e., coordination of HOHO···H—O$_{ice}$ type) is not feasible. The optimization of the corresponding structure results in the reorientation of H_2O_2 with the formation of an additional hydrogen bond with boundary atoms.

A two-fold coordinated complex at the side crystal plane can be formed with two neighboring dangling oxygen atoms or one neighboring dangling OH group and dangling oxygen atom. In both cases, the coordination of H_2O_2 does not break the O—H···O surface hydrogen bond. Moreover, the H_2O_2 adsorption even strengthens the hydrogen bond, acting like an additional bridge between two centers and decreasing the O—O distance. This results in an increase in the frequency of O—H vibrations of surface groups. The corresponding absorption bands of the H_2O_2 molecule, however, diminish. The binding energies corrected with BSSE and ZPE for these models are close to each other (27.2 and 25.9 kJ mol⁻¹) and are practically the same as in the case of the onefold coordinated model (26.8 kJ mol⁻¹).

The interaction of the H_2O_2 molecule with the basal plane of the ice *Ih* crystal surface results in the formation of multiple hydrogen bonds in the cluster with a binding energy of 28.5 kJ mol⁻¹. Frequency calculations show that two vibrations have strongly red-shifted frequencies of 3316 and 3374 cm⁻¹ (scaled frequencies are 3150 and 3205 cm⁻¹). Apart from these bands, there are two vibrations in the region 3400–3500 cm⁻¹

and the remaining OH valence modes are located in the region 3500–3750 cm^{-1}. The vibrational mode 3374 cm^{-1} has a large admixture of boundary OH groups, whereas the frequency 3316 cm^{-1} is almost completely assigned to the OH-stretching of a central, unfixed H_2O molecule between two dangling oxygen atoms where the H_2O_2 molecule is coordinated.

Based on the studies of vibrational frequencies of ice clusters with adsorbed H_2O_2 molecules, the conclusion was made[33] that the experimentally observed band 2860 cm^{-1} cannot be assigned to any vibration of coordinated OH groups of H_2O_2 or H_2O molecules. The effect of such a coordination in all the conformations under consideration is too small to shift the OH vibrations by 200–500 cm^{-1}. Thus, this band is assigned to the $\nu_2 + \nu_6$ combination band of H_2O_2 with an increased intensity because of crystal effects. A similar conclusion was also made by Engdahl et al. and Lundell et al.[71,72] in their analyses of the band structure of $(H_2O_2)_2$ and $H_2O_2 \cdot CO$ complexes. However, it should be noted that, as mentioned above, the intense bands of the $O(^1D)$ and HOO$^\bullet$ complexes formed on the ice surface are also located in the region 2800–3000 cm^{-1} and it cannot be excluded that these complexes can also contribute to the observed band at 2860 cm^{-1}.

The optimized structures for clusters representing the different modes of incorporation of H_2O_2 into the cluster body demonstrates that the H_2O_2 molecule forms three or four hydrogen bonds with neighboring water molecules. The ZPE-corrected binding energies of inclusion have small, positive values demonstrating that hydrogen bonds between H_2O_2 and the crystalline network are relatively weak and cannot compensate the energy of the structural distortion. It should be noted, however, that the boundary atoms of the cluster were fixed during the optimization. The calculated vibrational frequencies of such structures are only slightly distorted in comparison with the free H_2O_2 molecule. It is interesting to note that the effect of the electrostatic field investigated by Ignatov et al.[33] (in order to model the electrostatic potential of an infinite crystal) does not shift the OH vibrational bands of coordinated H_2O_2 significantly.

An experimental study of the interaction of H_2O_2 with an ice surface[107] demonstrates that the uptake of H_2O_2 molecules by the surface, driven by the formation of H-bonds, is small (a thousandth of a monolayer at 228 K and 10^{-4} Pa of H_2O_2 partial pressure) and scales linearly with partial pressure. These facts indicate that the binding energy of H_2O_2 at the ice surface is not high and dissociation does not occur. Thus, the experimental results support the picture of adsorption interaction obtained in theoretical studies.

It should be noted that the attempts to estimate the adsorption energy of H_2O_2 and other species on an ice surface clearly demonstrate a challenging problem that remains before modern computational chemistry. As mentioned in the Introduction, the ice *Ih* structure is defined by "ice rules".[108,109] In agreement with these, the only requirement imposed on the orientations of the H_2O molecules forming the lattice is that each water molecule should be bound by four hydrogen bonds O–H···O and the hydrogen atoms of a given molecule can occupy any two of them. This generates a large number of
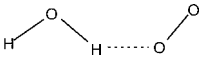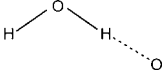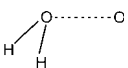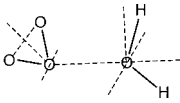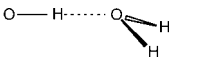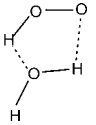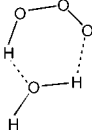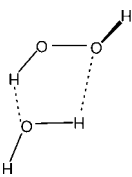
conformational isomers of crystal, the surfaces of which are distinguished by the orientations of the water molecules. Each of the surface conformations is characterized by its own (and frequently strongly distinguishing) binding energy relative to the adsorbed molecule. The number of possible conformations grows quickly with cluster size, becoming huge for any representative surface fragment. Unfortunately, all studies to date consider only several surface conformations (selected on the basis of the author's intuition on the possible contribution of a structure to the adsorption process), and there are no studies that try to estimate the impact of various structures in a systematic way. Obviously, at the very least, it is necessary to develop a practical procedure for a fast and cost-effective assessment and averaging of the adsorption energies for different conformations, which should probably be based on accurate calculations performed only for selected structures. Interesting results were recently obtained in this direction, using group theory to estimate the energy of cagelike water clusters.[110]

3. Conclusions and Outlook

The study of complexes involving water and inorganic atmospheric oxidants has a long history. Since the 1950s, when computational methods and matrix isolation became available, the structures of $H_2O \cdot O_3$, $H_2O \cdot HO^\bullet$, $H_2O \cdot HOO^\bullet$, and $H_2O \cdot H_2O_2$ have been studied by independent groups using different theoretical methods and can be considered today as well-established. However, it should be noted that, even among the well-established structures, revisions frequently occurred when a new experimental technique or a new, more sophisticated kind of theory, was applied (as took place for $H_2O \cdot O_3$ and $H_2O \cdot HO^\bullet$). Moreover, controversial observations are still taking place today, even for well-studied complexes and, thus, some doubts arise regarding the reliability of their structure. This holds for the complexes $H_2O \cdot HO^\bullet$, $H_2O \cdot O_3$, and $H_2O \cdot HOO^\bullet$. Two complexes $(H_2O \cdot O(^1D)$, $H_2O \cdot HOOO^\bullet)$ described in this review have so far not been observed experimentally. It should also be noted that the information about the structure of the $H_2O \cdot O_2$ complex cannot be considered as complete enough, primarily due to the very few studies performed so far. Moreover, the structure of complexes with molecular oxygen in the excited state has still not been studied, despite the obvious great importance of this species in the spectral balance of the atmosphere.

Table 4 summarizes the structure data and the binding energies of the binary complexes obtained at the most reliable levels of theory.

Regarding binding energies and related energetic parameters (D_0, ΔH etc.), significant discrepancies are observed. As a rule, most of the quantum chemical calculations described above no longer correspond to the modern level of computational chemistry and today's demands. In many studies, the binding energies were calculated using modest basis sets, without diffuse functions (which are extremely important for the weakly bound species) and without BSSE corrections (which are necessary to avoid large inaccuracies in the calculated binding energies). The most evident deficiency is a lack of high-level PES data suitable for the accurate estimation of ther-

Table 4. *Most reliable theoretical estimates of structural and energetic parameters of binary complexes of water with oxidant species.*

Complex	Molecular structure (most favorable conformation)	Structural parameters (bond lengths in Å)	Binding energy [kJ mol⁻¹]	Method of investigation, reference	Other studies
$H_2O \cdot O_2$	bent H-bonded structure	$R(H \cdots O) = 3.384$	$\Delta E = 3.1$ $\Delta E_{CP} = 2.3$	MP4(full)/6-311++G(2d,2p)//MP2(full)/6-311++G(2d,2p)[23]	refs. [22–25]
		$R(H \cdots O) = 3.226$	$\Delta E = 3.0$	QCISD/6-311++G(2d,2p)[24]	
$(H_2O \cdot O_2) \rightleftharpoons$ $(H_2O^+ \cdot O_2^-)$	van der Waals complex of $O-O \cdots H > O$ (bifurcating) C_{2v} structure charge-transfer complex— asymmetric twisted cyclic structure	$R(O-O \cdots OH_2) = 3.99$	$\Delta E = 3.60$ (van der Waals complex)	SCF, CI, DMA, MRSDCI[19] point-to-point optimization	refs. [16–21]
$(H_2O \cdot O_2) \rightleftharpoons$ $(H_2O^+ \cdot O_2^-)$	same as above			MP2(full)/6-311++G(2d,p) optimization CASSCF(10,7), MR-CISD, MR-ACPF energies	ref. [21]
$H_2O \cdot O(^3P)$	bent H-bonded structure	$R(H \cdots O) = 2.232$	$\Delta E_{CP} = 5.3$	UMP2/6-311++G(3d,3p)//UMP2/6-31G(d)[35]	refs. [34, 35]
$H_2O \cdot O(^1D)$	O—O-bonded structure	$R(O \cdots O) = 1.549$	$\Delta E = 155.2$	CCSD(T)/TZ2P+f[44]	refs. [38, 40–42, 45, 46]
$H_2O \cdot O_3$		$R(O \cdots O) = 2.906$	$\Delta E = 10.0$	QCISD(T)/6-311++3df,3pd)//QCISD/6-311++G(d,p))[51] MP4/6-31G(d,p)) partial optimization[47]	refs. [50, 51]
		$R(O \cdots O) = 2.965$	$\Delta E = 10.0$, $\Delta E_{CP} = 4.2$		
$H_2O \cdot HO$	H-bonded open structure	$R(O \cdots H) = 1.951$	$\Delta E = 23.8$	QCISD/6-311++G(2d,2p)[78]	refs. [73–80]
$H_2O \cdot HOO$	closed structure with two hydrogen bonds	$R(O \cdots H) = 1.789$ $R(H \cdots O) = 2.535$	$\Delta E = 40.2$ $D_0 = 29.3$	UMP2/6-311++G(2df,2p)[90]	refs. [88–91]
		$R(O-O \cdots OH_2) = 1.783$ $R(O-H \cdots O-O) = 2.406$	$\Delta E = 39.3$ $D_0 = 28.9$	CCSD(T)/6-311++G(2df,2p)//B3LYP/6-311++G(2df,2p)[90]	
$H_2O \cdot HOOO$	closed structure with two hydrogen bonds	$R(O \cdots H) = 1.782$ $R(H \cdots O) = 2.475$	$\Delta E = 33.5$	CCSD(T)/6-311++G(2df,2p)//B3LYP/6-311++G(3df,3pd)[98]	
$H_2O \cdot H_2O_2$		$R(H_2O \cdots HOOH) = 1.928$ $R(HOH \cdots O) = 2.213$	$\Delta E = 31.8$, $\Delta E_{CP} = 26.4$ $D_0 = 11.7$	MP2(Full)/6-311++G(2df,2pd)[101] MP2/6-311++G(3df,2p)[105]	refs. [89, 103–105]

modynamic function values. The estimates of the concentrations and their altitude profiles made on the basis of the presented studies cannot be considered as reliable enough and suitable for atmospheric studies.

Not enough is known about the transition from binary complexes to larger H_2O clusters and ice. Studies dedicated to the structure and energetics of the interaction of oxidant molecules with water in the series: binary complex—cluster—ice surface is still solitary, despite the clear importance of H_2O complexes and clusters in atmospheric science.

One can thus conclude that, despite the strong interest in water complexes with oxidant molecules in the atmosphere, our knowledge is still far from complete: further investigations, both theoretical and experimental, are required. On the basis of the present review, one can state that the most demanding directions of such studies are, first of all, the elaboration of high-level PES data needed to make accurate predictions of the thermodynamic parameters of weakly bound complexes and, thus, make predictions about their concentrations in different strata of the atmosphere. Another demanding question is the structure and reactivity of the adsorption complexes formed at the solid and liquid air–water interfaces whose role in the atmospheric processes is still poorly understood. New experimental techniques including time-resolved studies both in the gas phase and at the gas–solid interface could provide verification for theoretically proposed structures and reactivities of complexes involving oxidants and H_2O molecules or ice surfaces.

Acknowledgements

Keywords: atmospheric chemistry · cluster compounds · hydrogen bonds · ice surfaces · water chemistry

[1] Sh. Sh. Nabiev, P. G. Sennikov, *Opt. Atmos Okeana* **2001**, *14*, 189–210.
[2] V. Vaida, J. E. Headrick, *J. Phys. Chem. A* **2000**, *104*, 5401–5412.
[3] M. Staikova, D. J. Donaldson, *Phys. Chem. Earth C* **2001**, *26*, 473–478.
[4] J. E. Headrick, V. Vaida, *Phys. Chem. Earth C* **2001**, *26*, 479–486.
[5] K. R. Leopold, M. Canagaratna, J. A. Phillips, *Acc. Chem. Res.* **1997**, *30*, 57–64.
[6] J. S. Daniel, S. Solomon, R. W. Sanders, R. W. Portman, D. C. Miller, W. Madsen, *J. Geophys. Res.* **1999**, *104*, 16785–16791.
[7] Z. Slanina, F. Uhlik, A. T. Saito, E. Osawa, *Phys. Chem. Earth. C* **2001**, *26*, 505–511.
[8] C. Wittig, S. Sharpe, R. A. Beaudet, *Acc. Chem. Res.* **1988**, *21*, 341–347.
[9] G. Brasseur, S. Solomon, *Aeronomy of the Middle Atmosphere. Chemistry and Physics of the Stratosphere and Mesosphere*, D. Reidel Publishing Company, Dordrecht, **1986**, p. 198.
[10] B. J. Finlaysson-Pitts, J. N. Pitts, Jr., *Atmospheric Chemistry: Fundamentals and Experimental Techniques*, John Wiley and Sons, New York, **1986**.
[11] *Atmospheric Water Vapor* (Eds.: A. Deepack, T. D. Wilkerson, L. H. Ruhnke), Academic Press, New York, **1980**, p. 695.

[12] R. Goody, *Principles of Atmospheric Physics and Chemistry*, Oxford University Press, UK, **1995**.
[13] A. B. Horn, J. R. Sodeau, in *Water in Confining Geometries* (Eds.: V. Buch, J. P. Delvin), Springer Verlag, Berlin, **2003**, pp. 295–336.
[14] C. Girardet, C. Toubin, *Surf. Sci. Rep.* **2001**, *44*, 159–238.
[15] J. P. D. Abbatt, *Chem. Rev.* **2003**, *103*, 4783–4800.
[16] L. A. Curtiss, C. A. Melendres, *J. Phys. Chem.* **1984**, *88*, 1325–1329.
[17] A. E. Reed, F. Weinhold, L. A. Curtiss, D. J. Pochatko, *J. Chem. Phys.* **1986**, *84*, 5687–5705.
[18] E. S. Fois, A. Gamba, G. Morosi, P. Demontis, G. B. Suffritti, *J. Chim. Phys. Phys.-Chim. Biol.* **1987**, *84*, 751–754.
[19] W. B. Brown, M. A. Vincent, K. Trollope, I. H. Hillier, *Chem. Phys. Lett.* **1992**, *192*, 213–216.
[20] J. M. Seminario, M. C. Concha, J. S. Murray, P. Politzer, *Chem. Phys. Lett.* **1994**, *222*, 25–32.
[21] I. J. Palmer, W. Byers Brown, I. H. Hillier, *J. Chem. Phys.* **1996**, *104*, 3198–3204.
[22] W. B. Brown, *Chem. Phys. Lett.* **1995**, *235*, 94–98.
[23] I. M. Svishchev, R. J. Boyd, *J. Phys. Chem. A* **1998**, *102*, 7294–7296.
[24] T. W. Robinson, H. G. Kjaergaard, *J. Chem. Phys.* **2003**, *119*, 3717–3720.
[25] H. G. Kjaergaard, T. W. Robinson, D. L. Howard, J. S. Daniel, J. E. Headrick, V. Vaida, *J. Phys. Chem. A.* **2003**, *107*, 10680–10686.
[26] A. Sabu, S. Kondo, N. Miura, K. Hashimoto, *Chem. Phys. Lett.* **2004**, *391*, 101–105.
[27] Y. Kasai, Y. Sumiyoshi, Y. Endo, presented at *55th Int. Symp. on Molecular Spectroscopy*, The Ohio State University, Columbus, OH, **2000**. (Note these authors refer to the unpublished work of Y. Kasai on microwave spectroscopy of $H_2O \cdot O_2$ complex.)
[28] C. Muñoz-Caro, A. Niño, *J. Phys. Chem. A* **1997**, *101*, 4128–4135.
[29] J. S. Daniel, S. Solomon, *Geophys. Res. Lett.* **2004**, *31*, L06118.
[30] *IUPAC Subcommittee on Gas Kinetic Data Evaluation. Summary of Evaluated Kinetic and Photochemical Data for Atmospheric Chemistry*. Web version, November **2003**. http://www.iupac-kinetic.ch.cam.ac.uk Data Sheet POx1.
[31] S. H. Anderson, D. Hülsebusch, K. Mauersberger, *J. Chem. Phys.* **1997**, *107*, 5385–5392.
[32] *IUPAC Subcommittee on Gas Kinetic Data Evaluation. Summary of Evaluated Kinetic and Photochemical Data for Atmospheric Chemistry*. Web version, November **2003**. http://www.iupac-kinetic.ch.cam.ac.uk Data Sheet POx2.
[33] S. K. Ignatov, P. G. Sennikov, H.-W. Jacobi, A. G. Razuvaev, O. Schrems, *Phys. Chem. Chem. Phys.* **2003**, *5*, 496–505.
[34] L. Khriachtchev, M. Pettersson, S. Tuominen, M. Räsänen, *J. Chem. Phys.* **1997**, *107*, 7252–7259.
[35] S. Pehkonen, M. Pettersson, J. Lundell, L. Kriachtchev, M. Räsänen, *J. Phys. Chem. A* **1998**, *102*, 7643–7648.
[36] I. I. Moiseev, *J. Mol. Catal. A* **1997**, *127*, 1–23.
[37] O. Bain, P. A. Giguerre, *Can. J. Chem.* **1955**, *33*, 527-534.
[38] U. Kaldor, I. Shavitt, *J. Chem. Phys.* **1966**, *44*, 1823–1829.
[39] J. A. Pople, K. Raghavachari, M. J. Frisch, J. S. Binkley, P. v. R. Schleyer, *J. Am. Chem. Soc.* **1983**, *105*, 6389–6399.
[40] D. Cremer in *The Chemistry of Functional Groups, Peroxydes* (Ed.: S. Pataï), John Wiley and Sons, New York, **1983**, p. 36.
[41] R. D. Bach, J. J. W. McDouall, A. L. Owensby, H. B. Schlegel, *J. Am. Chem. Soc.* **1990**, *112*, 7065–7067.
[42] R. D. Bach, A. L. Owensby, C. Gonzalez, H. B. Schlegel, J. J. W. McDouall, *J. Am. Chem. Soc.* **1991**, *113*, 6001–6011.
[43] C. Meredith, T. P. Hamilton, H. F. Schaefer, *J. Phys. Chem.* **1992**, *96*, 9250–9254.
[44] H. H. Huang, Y. Xie, H. F. Schaefer, *J. Phys. Chem.* **1996**, *100*, 6076–6080.
[45] B. S. Jursic, *J. Mol. Struct. Theochem.* **1997**, *417*, 81–88.
[46] T. Okajima, *J. Mol. Struct. Theochem.* **2001**, *572*, 45–52.
[47] J. Z. Gillies, C. W. Gillies, R. D. Suenram, F. J. Lovas, T. Schmidt, D. Cremer, *J. Mol. Spectrosc.* **1991**, *146*, 493–512.
[48] A. Schriver, L. Schriver, C. Barreau, D. Carrière, J. P. Perchard, K. Jaeger, O. Schrems, in *Ozone in the Atmosphere: Proceedings of the Quadrennial Ozone Symposium 1988 and Tropospheric Ozone Workshop* (Eds.: R. D. Bojkov, P. Fabian), A. Deepak Publishing, **1989**, 694–697.
[49] L. Schriver, C. Barreau, A. Schriver, *Chem. Phys.* **1990**, *140*, 429–438.

[50] I. I. Zacharov, O. I. Kolbasina, T. N. Semenyuk, N. F. Tyupalo, G. M. Zhido-mirov, *Zh. Strukt. Khim.* **1993**, *34*, 26-30.

[51] H. Tachikava, S. Abe, *Inorg. Chem.* **2003**, *42*, 2188–2190.

[52] K. Jaeger, *Ph.D. Thesis*, University of Bremen, **1991**, 111–136.

[53] J. H. Seinfeld, S. N. Pandis, *Atmospheric Chemistry and Physics: From Air Pollution to Climate Change*, John Wiley and Sons: New York, **1998**.

[54] R. P. Wayne, *Chemistry of Atmospheres*, Clarendon Press, Oxford, **1991**.

[55] H. Chaabouni, L. Schriver-Mazzuoli, A. Schriver, *J. Phys. Chem. A* **2000**, *104*, 6962–6969.

[56] F. Borget, T. Chiavassa, A. Allouche, J. P. Aycard, *J. Phys. Chem. B* **2001**, *105*, 449–454.

[57] C. Manca, A. Allouche, *J. Chem. Phys.* **2001**, *114*, 4226–4234.

[58] R. D. Cess, M. H. Zhang, F. P. J. Valero, S. K. Pope, A. Bucholtz, B. Bush, C. S. Zender, J. Vitko Jr., *J. Geophys. Res.-Atmos.* **1999**, *104*, 2059–2066.

[59] J. T. Kiehl, J. J. Hack, M. H. Zhang, R. D. Cess, *J. Clim.* **1995**, *8*, 2200–2212.

[60] J. C. Hansen, J. S. Francisco, *ChemPhysChem* **2002**, *3*, 833–840.

[61] G. Frost, V. Vaida, *J. Geophys. Res.-Atmos.* **1995**, *100*, 18803–18809.

[62] S. Langenberg, U. Schurath, *Geophys. Res. Lett.* **1999**, *26*, 1695–1698.

[63] G. Brasseur, S. Solomon, *Aeronomy of the Middle Atmosphere*, 2nd ed., D. Reidel, **1997**.

[64] E. J. Dlugokencky, A. R. Ravishankara, *Geophys. Res. Lett.* **1992**, *19*, 41–44.

[65] M. T. Leu, *Geophys. Res. Lett.* **1988**, *15*, 851–854.

[66] J. A. Lannon, F. D. Verderame, R. W. Anderson Jr., *J. Chem. Phys.* **1971**, *54*, 2212–2223.

[67] N. Ackuista, L. T. Scoen, D. R. Lide Jr., *J. Chem. Phys.* **1968**, *48*, 1534–1536.

[68] B. M. Cheng, Y. P. Lee, J. F. Ogilvie, *Chem. Phys. Lett.* **1988**, *151*, 109–115.

[69] M. E. Jacox, D. E. Milligan, *J. Mol. Spectrosc.* **1972**, *42*, 495–513.

[70] A. J. Sedlacek, C. F. Wight, *J. Phys. Chem.* **1989**, *93*, 509–511.

[71] A. Engdahl, B. Nelander, G. Karlström, *J. Phys. Chem. A* **2001**, *105*, 8393–8398.

[72] J. Lundell, S. Jolkkonen, L. Khriachtchev, M. Pettersson, M. Räsänen, *Chem. Eur. J.* **2001**, *7*, 1670–1678.

[73] K. S. Kim, H. S. Kim, J. H. Jang, B.-J. Mhin, Y. Xie, H. F. Schaefer III, *J. Chem. Phys.* **1991**, *94*, 2057–2062.

[74] Y. Xie, H. F. Schaefer III, *J. Chem. Phys.* **1993**, *98*, 8829–8834.

[75] B. Wang, H. Hou, Y. Gu, *Chem. Phys. Lett.* **1999**, *302*, 96–100.

[76] V. S. Langford, A. J. McKinley, T. I. Quickenden, *J. Am. Chem. Soc.* **2000**, *122*, 12859–12863.

[77] P. D. Cooper, H. G. Kjaergaard, V. S. Langford, A. J. McKinley, T. I. Quickenden, D. P. Schofield, *J. Am. Chem. Soc.* **2003**, *125*, 6048–6049.

[78] A. Engdahl, G. Karlström, B. Nelander, *J. Chem. Phys.* **2003**, *118*, 7797–7802.

[79] A. Engdahl, B. Nelander, *J. Mol. Struct.* **1989**, *193*, 101–109.

[80] A. A. Nanyakkara, G. G. Balint-Kurti, I. H. Willians, *J. Phys. Chem.* **1992**, *96*, 3662–3669.

[81] S. Aloisio, J. S. Francisco, *Acc. Chem. Res.* **2000**, *33*, 825–830.

[82] B. Nelander, *J. Phys. Chem. A* **1997**, *101*, 9092–9096.

[83] E. J. Hamilton, *J. Chem. Phys.* **1975**, *63*, 3682–3683.

[84] R. A. Cox, J. P. Burrows, *J. Phys. Chem.* **1979**, *83*, 2560–2568.

[85] R. R. Lii, R. A. Grose, M. C. Sauer, S. Gordon, *J. Phys. Chem.* **1980**, *84*, 813–817.

[86] C. C. Kircher, S. P. Sander, *J. Phys. Chem.* **1984**, *88*, 2082–2091.

[87] D. R. Hanson, J. B. Burkholder, C. J. Howard, A. R. Ravishankara, *J. Phys. Chem.* **1992**, *96*, 4979–4985.

[88] E. J. Hamilton, C. A. Naleway, *J. Phys. Chem.* **1976**, *80*, 2037–2040.

[89] C. N. R. Rao, G. V. Kulkarni, A. M. Rao, U. C. Singh, *J. Mol. Struct. Theochem.* **1984**, *17*, 113–119.

[90] S. Aloisio, J. S. Francisco, *J. Phys. Chem. A* **1998**, *102*, 1899–1902.

[91] S. Aloisio, Yu. Li, J. S. Francisco, *J. Chem. Phys.* **1999**, *110*, 9017–9019.

[92] S. Aloisio, J. S. Francisco, R. R. Friedl, *J. Phys. Chem. A* **2000**, *104*, 6597–6601.

[93] R. A. Cox, J. P. Burrows, *J. Phys. Chem.* **1979**, *83*, 2560–2568.

[94] Q. Shi, S. D. Belair, J. S. Francisco, S. Kais, *Proc. Natl. Acad. Sci. USA* **2003**, *100*, 9686–9690.

[95] S. D. Belair, H. Hernandez, J. S. Francisco, *J. Am. Chem. Soc.* **2004**, *126*, 3024–3025.

[96] A. Morita, Yu. Kanaya, J. S. Francisco, *J. Geophys. Res.* **2004**, Doi:10.1029/2003 JD004240.

[97] S. D. Belair, S. Kais, J. S. Francisco, *Mol. Phys.* **2002**, *100*, 247–253.

[98] S. Aloisio, J. S. Francisco, *J. Am. Chem. Soc.* **1999**, *121*, 8592–8596.

[99] H. Kankaanpää, *Sedimentation, Distribution, Sources and Properties of Organic Material in Gulf of Finland*, Dissertation, Monograph of Borealis Environment Research, **1997**.

[100] T.-L. Tso, E. K. C. Lee, *J. Phys. Chem.* **1985**, *89*, 1612–1618.

[101] A. Engdahl, B. Nelander, *Phys. Chem. Chem. Phys.* **2000**, *2*, 3967–3970.

[102] G. C. M. van Duijneveldt-van de Riijdt, F. B. van Duijneveldt, *Chem. Phys.* **1993**, *175*, 271–281.

[103] J. A. Dobado, J. M. Molina, *J. Phys. Chem.* **1994**, *98*, 1819–1825.

[104] O. Mó, M. Yáñez, I. Rozas, J. Elguero, *Chem. Phys. Lett.* **1994**, *219*, 45–52.

[105] L. Gonzalez, O. Mo, M. Yáñez, *J. Comput. Chem.* **1997**, *18*, 1124–1135.

[106] X.-H. Ju, J.-J. Xiao, H.-M. Xiao, *J. Mol. Struct.-Theochem.* **2003**, *626*, 231–238.

[107] S. M. Clegg, J. P. D. Abbatt, *J. Phys. Chem. A* **2001**, *105*, 6630–6636.

[108] D. Bernal, R. H. Fowler, *J. Chem. Phys.* **1933**, *1*, 515–548.

[109] L. Pauling, *J. Am. Chem. Soc.* **1935**, *57*, 2680–2684.

[110] J.-L. Kuo, J. V. Coe, Sh. J. Singer, Y. B. Band, L. Ojamäe, *J. Chem. Phys.* **2001**, *114*, 2527–2540.